

# Training on the test set? An analysis of Spampinato et al. [31]

Ren Li, Jared S. Johansen, Hamad Ahmed, Thomas V. Ilyevsky, Ronnie B Wilbur, Hari M Bharadwaj, and Jeffrey Mark Siskind, *Senior Member, IEEE*

**Abstract**—A recent paper [31] claims to classify brain processing evoked in subjects watching ImageNet stimuli as measured with EEG and to employ a representation derived from this processing to construct a novel object classifier. That paper, together with a series of subsequent papers [8, 15, 17, 20, 21, 30, 35], claims to revolutionize the field by achieving extremely successful results on a wide variety of computer-vision tasks, including object classification, transfer learning, and generation of images depicting human perception and thought using brain-derived representations measured through EEG. Our novel experiments and analyses demonstrate that their results crucially depend on the block design that they employ, where all stimuli of a given class are presented together, and fail with a rapid-event design, where stimuli of different classes are randomly intermixed. The block design leads to classification of arbitrary brain states based on block-level temporal correlations that tend to exist in all EEG data, rather than stimulus-related activity. Because every trial in their test sets comes from the same block as many trials in the corresponding training sets, their block design thus leads to surreptitiously training on the test set. This invalidates all subsequent analyses performed on this data in multiple published papers and calls into question all of the purported results. We further show that a novel object classifier constructed with a random codebook performs as well as or better than a novel object classifier constructed with the representation extracted from EEG data, suggesting that the performance of their classifier constructed with a representation extracted from EEG data does not benefit at all from the brain-derived representation. Our results calibrate the underlying difficulty of the tasks involved and caution against sensational and overly optimistic, but false, claims to the contrary.

**Index Terms**—object classification, EEG, neuroimaging

## 1 INTRODUCTION

A recent paper [31] claims to (learn to) classify EEG data recorded from human subjects observing images from ImageNet [7] and use the learned classifier to train a pure computer-vision model. In that paper, images from ImageNet are presented as stimuli to human subjects undergoing EEG and a long short-term memory (LSTM [12]), combined with a fully connected layer and a ReLU layer, is trained to predict the class of the stimulus from the recorded EEG signal. The output of the ReLU layer is taken to reflect human neural encoding of the percept. The output of existing object classifiers is then regressed to this purported human neural encoding of the percept in an attempt to have computer-vision systems produce the same encoding of the percept.

That paper makes three specific claims [31, § 1 p. 6810]:

1. *We propose a deep learning approach to classify EEG data evoked by visual object stimuli outperforming state-of-the-art methods both in the number of tackled object classes and in classification accuracy.*
2. *We propose the first computer vision approach driven by brain signals, i.e., the first automated classification approach employing visual descriptors extracted*

*directly from human neural processes involved in visual scene analysis.*

3. *We will publicly release the largest EEG dataset for visual object analysis, with related source code and trained models.*

In particular, regarding claim 1, that paper further claims:

- i. Their method can classify a far larger number (40) of distinct object classes than prior work (at most 12 [13], typically 2) on classifying EEG signals.
- ii. Their method achieves far higher accuracy (82.9%) than prior work [13] (29%) on classifying EEG signals.

That paper further couches its purported results in superlatives:

*In this paper, we want to take a great leap forward with respect to classic BCI approaches, i.e., we aim at exploring a new and direct form of human involvement (a new vision of the “human-based computation” strategy) for automated visual classification. The underlying idea is to learn a brain signal discriminative manifold of visual categories by classifying EEG signals—reading the mind—and then to project images into such manifold to allow machines to perform automatic visual categorization—transfer human visual capabilities to machines. The impact of decoding object category-related EEG signals for inclusion into computer vision methods is tremendous. First, identifying EEG-based discriminative features for visual categorization might provide meaningful insight about the human visual perception systems. As a consequence, it will greatly advance performance of BCI-based applications as well*

All authors are with Purdue University, West Lafayette, IN 47907 USA. R. Li, J. S. Johansen, H. Ahmed, T. V. Ilyevsky and J. M. Siskind are with the School of Electrical and Computer Engineering. R. B. Wilbur is with the Department of Speech, Language, and Hearing Sciences and the Linguistics Program. H. M. Bharadwaj is with the Weldon School of Biomedical Engineering and the Department of Speech, Language, and Hearing Sciences. E-mail: li2515@purdue.edu, jjohanse@purdue.edu, ahmed90@purdue.edu, tilyevsk@purdue.edu, wilbur@purdue.edu, hbharadwaj@purdue.edu, qobi@purdue.edu  
Manuscript received

*as enable a new form of brain-based image labeling. Second, effectively projecting images into a new biologically based manifold will change radically the way object classifiers are developed (mainly in terms of feature extraction).* [31, § 1 pp. 6809–6810]

Here, we report a number of experiments and analyses that call these results and claims into question. Specifically, we find that the classifier employed makes extensive, if not sole, use of long-term static brain activity that persists much longer than the duration of individual stimuli. Since the paper employs a block design, where all stimuli of a given class are presented to a subject in succession, the classifiers employed tend to classify the brain activity during that block, which appears to be largely uncorrelated with stimulus class. This is exacerbated by the reliance of the classifier on DC and very-low frequency (VLF) components in the EEG signal that reflect arbitrary long-term static mental states during a block rather than dynamic brain activity. Since each trial in the test sets employed comes from the same block as many trials in the corresponding training sets, the reported high classification accuracy results from surreptitious training on the test set. When the experiment is repeated with a rapid-event design, where stimuli of different classes are randomly intermixed, classification accuracy drops to chance. As a result, this renders suspect all of the results and claims advanced in multiple published papers [8, 15, 17, 20, 21, 30, 31, 35]. Our experiments suggest that the underlying tasks are far more difficult than they appear on the surface and are far beyond the current state of the art. This suggests caution in light of widely published [8, 15, 17, 20, 21, 30, 31, 35] sensational claims that are overly optimistic but false.

## 2 OVERVIEW

In § 3, we report a comprehensive set of experiments and analyses to fully understand the results and claims reported by Spampinato et al. [31]. We first summarize our findings:

- a. In § 3.3, we reanalyze the EEG data collected by Spampinato et al. [31] using a number of different classifiers in addition to the one based on an LSTM that was employed by Spampinato et al. [31]. We show that one can obtain good, if not better, results with other classifiers, particularly ones that are sensitive to temporal alignment, unlike LSTMs. When we further reanalyze the EEG data collected by Spampinato et al. [31] with shorter temporal windows (as short as a single temporal sample), with random temporal offset, and with a reduced set of channels, we obtain even better results with these different classifiers. This suggests that the data collected by Spampinato et al. [31] lacks temporal and detailed spatial information reflective of perceptual processes that would benefit classification.
- b. In § 3.4, we replicate the data collection effort of Spampinato et al. [31] using the same stimuli, presentation order, and timing, recording 96 channels with finer quantization (24 *vs.* 16 bits) and higher temporal sampling rate (4096 Hz *vs.* 1 kHz). We do this both with the original block design employed by Spampinato et al. [31], where all stimuli of a given class are presented together, and with a rapid-event design, where stimuli of different classes are randomly intermixed. We also collect data with both the block and rapid-event designs, both for the original still-image stimuli depicting objects from ImageNet and short video clips depicting activity classes from Hollywood 2 [18].
- c. In § 3.5, we replicate all of the analyses of § 3.3 on our new data. For data collected with the block design, we obtain moderately good classification accuracy on both image and video stimuli with one classifier, long windows, and a large set of channels. However, we obtain poor classification accuracy with all of the other classifiers, shorter windows, and a small set of channels. We further find that all classifiers yield chance performance on data collected with a rapid-event design.
- d. Spampinato et al. [31] state that their data analysis included notch and bandpass filtering. Thus the analyses in § 3.5 employed such filtering, which removes the DC and VLF components. Since Palazzo [19] and Spampinato [26] indicated to us in email (§ 4.1) that they did not perform bandpass filtering, in § 3.6, we repeat the analysis of our data without bandpass filtering as well. Retaining the DC and VLF component allows us to replicate the results obtained on the data released by Spampinato et al. [31] with our data collected with a block design. However, we still obtain chance for our data collected with a rapid-event design.
- e. The block design employed by Spampinato et al. [31], together with their splits, has the property that every trial in each test set comes from a block that contains many trials in the corresponding training set. In § 3.7, we conduct three new analyses. In the first new analysis, we repeat the analysis on the data released by Spampinato et al. [31] using new splits where the trials in each test set come from blocks that do not contain trials in the corresponding training set. Classification accuracy drops to chance. In the second new analysis, we repeat the analysis on our new data collected with a rapid-event design, where the labels are replaced with block-level labels instead of stimulus-level labels. Classification accuracy rises from chance to levels far above chance, reaching those obtained on the data collected by Spampinato et al. [31]. In the third new analysis, we rerun the code released by Spampinato et al. [31] on the data released by Spampinato et al. [31] after first applying various highpass filters to the data. Classification accuracy drops from roughly 93% to roughly 32%. Collectively these demonstrate that the high classification accuracies reported by Spampinato et al. [31] result from classifying the long-term brain activity associated with a block, even when that block contains stimuli of different classes, not the brain activity associated with perception of the class of the stimuli. They further demonstrate that this is exacerbated by the presence of DC and VLF components of the signal that remain due to lack of bandpass filtering. This refutes claims 1 and 3.
- f. In § 3.8 and § 3.9, we replicate the regression and transfer-learning analyses performed by Spampinato et al. [31, § 3.3, § 4.2, and § 4.3] but with a twist. We replace the EEG encodings with a random codebook and achieve equivalent, if not better, results. This demonstrates that the regression and transfer-learning analyses performed

by Spampinato et al. [31] are not benefiting from a brain-inspired or brain-derived representation in any way, refuting claim 2.

### 3 EXPERIMENTS

Our findings in § 5 and § 6 are supported by the following experiments and analyses performed.

#### 3.1 The Spampinato et al. [31] data collection

Spampinato et al. [31] adopted the following experimental protocol. They selected 40 object classes from ImageNet [31, footnote 1] along with 50 images for each class. These were presented as stimuli to 6 human subjects undergoing EEG. A block design was employed. Each subject saw 40 blocks, each containing 50 image stimuli. Each image was presented exactly once. All 50 stimuli in a block were images of the same class. All subjects saw exactly the same 2,000 images. We do not know whether different subjects saw the classes, or the images in a class, in different orders. The image presentation order for one subject was provided to us by the authors. Each image was presented for 0.5 s. Blocks were separated by 10 s of blanking. Approximately  $40 \times (50 \times 0.5 \text{ s} + 10 \text{ s}) = 1400 \text{ s}$  of EEG data were collected from 128 channels at 1 kHz with 16 bit resolution.

#### 3.2 The Spampinato et al. [31] data analysis

Spampinato et al. [31] report that the EEG data was pre-processed by application of a notch filter (49–51 Hz) and a second-order band-pass Butterworth filter (low cutoff frequency 14 Hz, high cut-off frequency 71 Hz). The pass band was selected to include the *Beta* (15–31 Hz) and *Gamma* (32–70 Hz) bands, as they convey information about the cognitive processes involved in the visual perception [31, § 3.1 p. 6812]. The data for all 6 subjects was pooled, segmented into trials of approximately 0.5 s duration, and divided into six training/validation/test-set splits. Each portion of each split contained data from all 6 subjects and all classes for all subjects. The data was z-scored prior to training and classification. An LSTM, combined with a fully connected layer and a ReLU layer, was applied to a 440 ms window of each trial starting 40 ms from stimulus onset. A variety of different architectural parameters were evaluated, the best of which achieved 85.4% validation accuracy and 82.9% test accuracy. Spampinato et al. [31] claim that this is significantly higher classification accuracy for a significantly larger number of classes than all prior reported classification experiments on EEG data [2–5, 13, 23, 33, 34, 36].

#### 3.3 Reanalysis of the Spampinato et al. [31] data

We asked whether the significant improvement in classification ability was due to the classifier architecture employed by Spampinato et al. [31] or whether it was due to some aspect of their experimental protocol and data collection procedure. Spampinato et al. [31] have publicly released their code<sup>1</sup> and data.<sup>2</sup> This allowed us to verify their

TABLE 1

Classification accuracy averaged across validation sets, test sets, and all 6 splits used by Spampinato et al. [31] on their released data with their software (an LSTM combined with a fully connected layer and a ReLU layer) and four new classifiers: a nearest neighbor classifier ( $k$ -NN), an SVM, an MLP, and a 1D CNN.

LSTM	$k$ -NN	SVM	MLP	1D CNN
93.7%	42.9%	94.0%	49.0%	97.4%

published results and to reanalyze their data with different classifiers to investigate this question. The released code yields (slightly better than) the published accuracy on the released data.

Spampinato et al. [31] have released their data in both Python and Matlab formats. Both formats are subsequent to segmentation. All results reported here were produced with the Python format data which was z-scored before processing. See § 4 for details.

We reanalyzed the Spampinato et al. [31] data with four different classifiers (Table 1): a  $k$ -nearest neighbor classifier ( $k$ -NN), a support vector machine (SVM [6]), a multilayer perceptron (MLP), and a 1D convolutional neural network (CNN).<sup>3</sup> The  $k$ -nearest-neighbor classifier used  $k = 7$  with a Euclidean distance on the  $128 \times 440 = 56320$  element vector associated with each trial. The SVM employed a linear kernel applied to data that was temporally down-sampled to 500 Hz, *i.e.*,  $128 \times 220 = 28160$  element vectors. The MLP employed two fully connected layers with a sigmoid activation function after the first fully connected layer, and no dropout, trained with a cross-entropy loss, applied to  $128 \times 440 = 56320$  element vectors, with 128 hidden units. The 1D CNN (Fig. 1) processed each of the 128 channels independently with eight 1D CNNs of length 32 and stride 1. The 128 applications of each of the eight 1D CNNs shared the same parameters. The output of each was processed by an ELU, followed by dropout with probability of 0.5. This yielded a temporal feature stream of length  $440 - 32 + 1 = 409$  with  $128 \times 8 = 1024$  features per time point. This was then processed by a fully connected layer mapping each time point to a 40 element vector. The parameters were shared across all time points. This was then processed by average pooling along the time axis, independently for each of the 40 channels, with a kernel of length 128 and a stride of 64. This produced a feature map with 40 features for 5 time points. Dropout with probability 0.5 was then applied, followed by a fully connected layer with 40 outputs. Training was performed with a cross-entropy loss.

The results in Table 1 suggest that there is nothing specific about the classifier architecture employed by Spampinato et al. [31] that yields high results. The same results can be obtained not only with an LSTM-based classifier or a 1D CNN that attempts to model the temporal nature of the signal, but also with an SVM that has no particular temporal structure. Moreover, while other methods such as  $k$ -NN and MLP that also lack temporal structure do not yield as high accuracy, they nonetheless yield accuracy far

<sup>1</sup>[http://perceive.dieei.unict.it/files/cvpr\\_2017\\_eeg\\_encoder.py](http://perceive.dieei.unict.it/files/cvpr_2017_eeg_encoder.py)

<sup>2</sup>[http://perceive.dieei.unict.it/index-dataset.php?name=EEG\\_Data](http://perceive.dieei.unict.it/index-dataset.php?name=EEG_Data)

<sup>3</sup>All code and data needed to replicate the results in this paper are available at <https://github.com/qobi/tpami2019>.

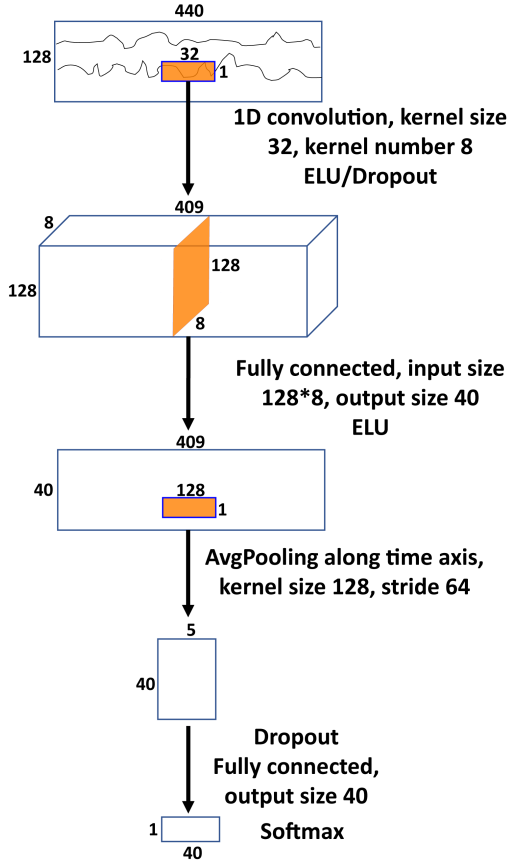


Fig. 1. Our 1D CNN used to process EEG data.

TABLE 2

Classification accuracy for varying trial window lengths with random temporal offset from the stimulus onset, averaged across validation sets, test sets, and all 6 splits used by Spampinato et al. [31] on their data with all 5 classifiers.

window	LSTM	$k$ -NN	SVM	MLP	1D CNN
200 ms	93.4%	39.5%	93.7%	62.9%	97.4%
100 ms	95.1%	39.5%	93.5%	77.4%	n/a
50 ms	96.3%	39.1%	93.7%	85.9%	n/a
1 ms	92.9%	43.3%	90.3%	92.1%	n/a

higher than chance and far higher than any of the results reported in the literature cited by Spampinato et al. [31]: [2–5, 13, 23, 33, 34, 36].

Given that high accuracy was achieved with classifiers that should be sensitive to temporal translation of the signal, we asked whether the classification accuracy depended on this. To this end, we trained and tested all 5 classifiers, varying the length of the trial window between 200 ms, 100 ms, 50 ms, and 1 ms (Table 2).<sup>4</sup> In all cases, the trial window was started at a random offset from the stimulus onset, on a trial-by-trial basis. Note that high accuracy can even be obtained with a single temporal sample randomly selected within the stimulus interval. This suggests that no temporal brain processing is reflected in the classification accuracy.

<sup>4</sup>Due to the nature of its design, the 1D CNN model was never applied to windows shorter than 200 ms.

An earlier report [30] conducted a similar data collection effort to that of Spampinato et al. [31] with 32 channels instead of 128. That effort yielded considerably lower classification accuracy (about 40%) on the same classes, stimuli, experimental protocol, and classification architecture. Given that the classifiers analyzed here appear not to rely on the temporal nature of brain processing, we asked how much they rely on the number of channels. To this end, we performed feature *i.e.*, channel selection on the dataset to train and test with various subsets of channels of different sizes. The Fisher score [11] of a channel  $v$  for a classification task with  $C$  classes where each class  $c$  has  $n_c$  examples was computed as

$$\frac{\sum_{c=1}^C n_c (\mu_{c,v} - \mu_v)^2}{\sum_{c=1}^C n_c \sigma_{c,v}^2} \quad (1)$$

where  $\mu_{c,v}$  and  $\sigma_{c,v}$  were the per-class per-channel means and variances and  $\mu_v$  was the per-channel mean. We selected the  $m$  channels with highest Fisher score on the training set, for varying  $m$ , and repeated the training and testing on this subset of channels for varying window lengths (Table 3). We observe that the full 128 channels are not necessary to achieve high accuracy. While the accuracy degrades somewhat when using fewer than 32 channels, one can obtain far greater accuracy than chance and far greater accuracy than all prior reported classification experiments cited by Spampinato et al. [31]: [2–5, 13, 23, 33, 34, 36] on EEG data with as few as 8 channels. Moreover, one can obtain far greater accuracy than Spampinato et al. [30] with the same number (32) of channels and the same accuracy with far fewer (8) channels. While the spatial layout of channel selection might not coincide with the electrode placement of a cap with fewer electrodes, we next discuss why we consider it important that one can accurately classify the Spampinato et al. [31] data with such extreme spatial and temporal downsampling.

### 3.4 New data collection

The above analyses suggest that the accuracy achieved by Spampinato et al. [31] was not due to the analysis architecture but rather due to either the experimental protocol or the data collection effort. We asked whether the accuracy was due to the former or the latter. To this end, we repeated the data collection effort four times, all with the same single subject. The first two used the same 40 object classes and 2,000 image stimuli as Spampinato et al. [31]. The second two used the 12 activity classes and a subset of the video clips from Hollywood 2 as described in Siskind [25]. The subset of clips was selected to be counterbalanced, with 32 clips per class, temporally cropped to a uniform 4 s duration centered around the activity class depicted, and transcoded to a uniform spatial and temporal resolution. Data was collected twice for each set of stimuli. One collection used a block design, where all stimuli of a given class were shown together in a single block. The other collection used a rapid-event design, where the stimuli were presented in randomized order. The block design for the image stimuli employed

TABLE 3

Classification accuracy for varying numbers of channels, averaged across validation sets, test sets, and all 6 splits used by Spampinato et al. [31] on their data with all 5 classifiers and varying trial window lengths with random temporal offset from the stimulus onset.

window	channels	LSTM	<i>k</i> -NN	SVM	MLP	1D CNN
440 ms	96	96.1%	45.4%	95.3%	62.7%	97.6%
200 ms	96	95.4%	42.2%	94.7%	77.2%	97.8%
100 ms	96	96.4%	42.7%	94.4%	84.8%	n/a
50 ms	96	95.8%	41.3%	94.4%	90.6%	n/a
1 ms	96	92.9%	49.5%	90.4%	93.0%	n/a
440 ms	64	96.5%	55.4%	95.9%	76.8%	97.1%
200 ms	64	96.4%	52.6%	95.0%	86.1%	97.5%
100 ms	64	96.1%	52.4%	95.2%	90.3%	n/a
50 ms	64	97.7%	52.5%	95.0%	93.3%	n/a
1 ms	64	92.8%	61.8%	90.2%	93.2%	n/a
440 ms	32	53.8%	58.4%	83.6%	85.6%	89.5%
200 ms	32	91.1%	55.8%	81.0%	88.3%	90.2%
100 ms	32	92.3%	55.8%	80.7%	90.3%	n/a
50 ms	32	93.9%	55.1%	80.1%	90.5%	n/a
1 ms	32	79.5%	62.3%	68.0%	81.6%	n/a
440 ms	24	56.9%	56.4%	72.0%	82.7%	82.2%
200 ms	24	80.0%	53.3%	67.7%	83.5%	82.3%
100 ms	24	91.8%	53.4%	67.4%	84.7%	n/a
50 ms	24	92.8%	52.7%	66.5%	86.6%	n/a
1 ms	24	74.9%	58.7%	54.6%	73.0%	n/a
440 ms	16	38.5%	57.1%	54.5%	78.7%	70.1%
200 ms	16	57.5%	54.5%	49.6%	79.0%	68.9%
100 ms	16	84.5%	54.1%	48.3%	79.4%	n/a
50 ms	16	81.8%	53.3%	47.5%	79.2%	n/a
1 ms	16	62.4%	55.8%	39.5%	61.5%	n/a
440 ms	8	24.6%	48.1%	22.8%	57.8%	41.6%
200 ms	8	45.0%	45.4%	18.6%	57.6%	41.4%
100 ms	8	64.8%	44.5%	17.5%	57.9%	n/a
50 ms	8	66.3%	44.0%	18.0%	59.5%	n/a
1 ms	8	43.5%	42.9%	16.9%	37.9%	n/a

the same design as Spampinato et al. [31]: 40 blocks, each consisting of 50 stimuli, each presented for 0.5 s with 10 s of blanking after each block. The presentation order of the classes and stimuli within each class were the same as in the data collected by Spampinato et al. [31]. The rapid-event design for the image stimuli also employed 40 blocks, each consisting of 50 stimuli, each presented for 0.5 s with 10 s of blanking after each block, just that each block contained a random selection of images from different classes. In the latter, different blocks could contain different numbers of images for different classes, subject to the constraint that, over the entire experiment, each of the 2,000 images was shown exactly once. The block design for the video stimuli began with 8 s of fixation blanking, followed by 12 blocks, during each of which 32 clips were presented in succession, each lasting 4 s, with 10 s of fixation blanking after each block. Approximately  $12 \times (32 \times 4 \text{ s} + 10 \text{ s}) = 1656 \text{ s}$  of EEG data were collected. For the block design, all stimuli within the block were of the same class. The rapid-event design for the video stimuli also employed 12 blocks, each consisting of 32 stimuli, each presented for 4 s with 10 s of blanking after each block, just that each block contained a random selection of clips from different classes. In the latter, different blocks could contain different numbers of clips for different classes, subject to the constraint that, over the entire experiment, each of the 384 clips was shown exactly once. Unlike the data collection effort of Spampinato et al. [31], which divided each recording into four 350 s sessions, each of our four recordings was collected in a single session.

EEG data was recorded from 96 channels at 4096 Hz with

24 bit resolution using a BioSemi ActiveTwo recorder<sup>5</sup> and a BioSemi gel electrode cap. Two additional channels were used to record the signal from the earlobes for rereferencing. A trigger was recorded in the EEG data to indicate stimulus onset. We downsampled the data to 1.024 kHz, rereferenced the data to the earlobes, and employed the same preprocessing as reported by Spampinato et al. [31]: a band-pass filter (low cutoff frequency 14 Hz, high cut-off frequency 71 Hz), a notch filter (49–51 Hz), and z-scoring.<sup>6</sup>

### 3.5 Analysis of our new data

We applied the analysis from Table 3 to our new data collected with the block design for the image (Table 4 left) and video (Table 4 right) stimuli. This subsumes all analyses performed on the Spampinato et al. [31] data. Note that we are not able to replicate the results of Spampinato et al. [31]. While the 1D CNN achieves moderately good performance on both image and video stimuli, the other classifiers perform poorly. Moreover, for shorter analysis windows, random offsets, and reduced numbers of channels, the other classifiers perform largely at chance. We analyze the source of this difference below.

We then applied all of the classifiers from Table 1 to the data collected with a rapid-event design for the image (Table 5 left) and video (Table 5 right) stimuli. Note that all classifiers yield chance performance.

### 3.6 Spectral analysis

We asked why it is possible to achieve high accuracy with short analysis windows on the Spampinato et al. [31] data but not with our data. Palazzo [19] and Spampinato [26] indicated to us in email that their report of preprocessing was a misprint and that they performed notch filtering (during acquisition) and z-scoring but not bandpass filtering. See § 4.1 for details. Since their released code performs z-scoring, this indicates that their released data reflects notch filtering but neither bandpass filtering nor z-scoring. We thus reanalyzed our data with a notch filter and z-scoring but no bandpass filter (Tables 6 and 7). Note that we now obtain better results for the data collected with the block design, similar to that obtained with the data released by Spampinato et al. [31], but still obtain chance for data collected with the rapid-event design.

### 3.7 Block vs. Rapid-Event Design

We asked why we (and Spampinato et al. [31]) are able to obtain high classification accuracy with a block design but not a rapid-event design. To this end, we performed three reanalyses. First, we repeated the analysis from Tables 1–3, where instead of using the training/test set splits provided by Spampinato et al. [31], we conducted a leave-one-subject-out round-robin cross validation, training on all data from

<sup>5</sup>The ActiveTwo recorder employs  $64\times$  oversampling and a sigma-delta A/D converter, yielding less quantization noise than 24 bit uniform sampling.

<sup>6</sup>Spampinato et al. [31] presumably applied a notch filter to remove 50 Hz line noise. Being in the US, we should nominally remove 60 Hz line noise instead of 50 Hz. However, after rereferencing, our data contains no line noise so notch filtering is unnecessary. We employ a 50 Hz notch filter just to replicate Spampinato et al. [31].

TABLE 4

Application of the analysis from Table 3 to our new data collected with a block design on (left) image and (right) video stimuli, where our new data has been preprocessed with bandpass filtering.

window	channels	LSTM	$k$ -NN	SVM	MLP	1D CNN	window	channels	LSTM	$k$ -NN	SVM	MLP	1D CNN
440 ms	96	22.4%	2.5%	4.5%	4.9%	60.5%	4000 ms	96	13.3%	8.3%	8.3%	12.0%	65.9%
200 ms	96	20.5%	3.0%	3.3%	3.2%	53.8%	2000 ms	96	15.6%	7.0%	10.4%	7.3%	66.7%
100 ms	96	20.8%	3.2%	3.9%	3.7%	n/a	1000 ms	96	14.8%	9.6%	8.9%	10.9%	64.3%
50 ms	96	12.9%	3.7%	3.2%	3.8%	n/a	500 ms	96	12.2%	6.3%	7.0%	6.8%	n/a
1 ms	96	5.2%	5.3%	3.7%	3.8%	n/a	1 ms	96	13.8%	9.9%	9.1%	9.6%	n/a
440 ms	64	20.0%	2.9%	4.8%	4.1%	53.0%	4000 ms	64	10.9%	7.3%	9.4%	10.9%	62.5%
200 ms	64	11.2%	2.6%	3.0%	2.9%	40.7%	2000 ms	64	10.7%	7.8%	9.9%	9.1%	65.1%
100 ms	64	9.6%	3.3%	3.4%	3.3%	n/a	1000 ms	64	13.3%	7.8%	10.7%	8.3%	64.1%
50 ms	64	8.9%	3.8%	2.9%	2.9%	n/a	500 ms	64	12.0%	7.8%	8.9%	9.6%	n/a
1 ms	64	6.1%	4.4%	3.1%	4.3%	n/a	1 ms	64	8.6%	9.9%	8.1%	10.1%	n/a
440 ms	32	9.9%	3.3%	4.0%	3.7%	34.4%	4000 ms	32	9.4%	9.4%	13.5%	12.0%	51.6%
200 ms	32	8.4%	2.4%	3.3%	3.0%	24.7%	2000 ms	32	12.5%	7.3%	8.1%	9.9%	61.7%
100 ms	32	7.7%	2.6%	3.0%	2.5%	n/a	1000 ms	32	12.2%	9.9%	10.7%	9.6%	52.6%
50 ms	32	6.2%	3.3%	4.1%	3.4%	n/a	500 ms	32	12.0%	4.9%	8.1%	8.9%	n/a
1 ms	32	4.7%	4.2%	3.3%	3.4%	n/a	1 ms	32	14.8%	9.4%	11.2%	11.5%	n/a
440 ms	24	8.3%	3.1%	4.1%	3.6%	27.7%	4000 ms	24	8.3%	7.3%	11.5%	9.9%	40.1%
200 ms	24	7.9%	2.1%	3.4%	3.3%	27.3%	2000 ms	24	8.6%	7.8%	7.3%	7.6%	52.6%
100 ms	24	6.3%	2.2%	2.8%	2.5%	n/a	1000 ms	24	9.9%	9.9%	8.3%	7.6%	44.5%
50 ms	24	6.3%	2.8%	3.5%	2.2%	n/a	500 ms	24	13.5%	6.8%	9.6%	9.6%	n/a
1 ms	24	5.0%	4.4%	3.6%	3.8%	n/a	1 ms	24	9.4%	6.3%	10.2%	9.6%	n/a
440 ms	16	6.7%	2.4%	3.8%	3.2%	22.5%	4000 ms	16	9.6%	10.4%	10.4%	9.6%	44.8%
200 ms	16	6.9%	2.6%	2.5%	2.9%	19.0%	2000 ms	16	11.5%	7.3%	7.3%	6.5%	47.9%
100 ms	16	4.9%	2.5%	2.7%	3.1%	n/a	1000 ms	16	7.8%	9.9%	9.6%	8.9%	41.1%
50 ms	16	5.7%	2.6%	2.9%	3.2%	n/a	500 ms	16	11.2%	7.3%	10.7%	7.3%	n/a
1 ms	16	5.7%	3.7%	2.7%	3.7%	n/a	1 ms	16	9.4%	12.0%	6.0%	9.9%	n/a
440 ms	8	5.8%	2.9%	4.2%	3.5%	15.2%	4000 ms	8	9.1%	8.3%	10.4%	9.1%	26.6%
200 ms	8	5.2%	2.7%	3.1%	2.6%	13.8%	2000 ms	8	12.2%	8.6%	7.0%	10.4%	35.2%
100 ms	8	5.4%	2.7%	3.5%	2.5%	n/a	1000 ms	8	8.9%	7.0%	9.1%	6.8%	26.8%
50 ms	8	4.8%	3.5%	3.3%	3.2%	n/a	500 ms	8	11.2%	8.3%	9.9%	8.9%	n/a
1 ms	8	4.9%	3.6%	2.7%	3.7%	n/a	1 ms	8	10.9%	12.2%	10.7%	10.4%	n/a

TABLE 5

Application of the analysis from Table 1 to our new data collected with a rapid-event design on (left) image and (right) video stimuli, where our new data has been preprocessed with bandpass filtering.

LSTM	$k$ -NN	SVM	MLP	1D CNN	LSTM	$k$ -NN	SVM	MLP	1D CNN
2.9%	2.7%	3.4%	2.7%	2.1%	8.3%	13.5%	7.3%	6.3%	10.4%

five of the subjects and testing on all data from the sixth, rotating among all six subjects as test (Table 8). Note that classification accuracy is now at chance.

Second, we reran all of the analyses from Table 6 on our new data collected with a rapid-event design, both with and without bandpass filtering, but with a twist. Instead of using correct labels, which varied on a stimulus-by-stimulus basis, we used random labels, which varied on a block-by-block basis: each block was given a distinct label but all stimuli within a block were given the same label. Thus while the stimuli are changing in each block, they are given the wrong unchanging label and, like the block design employed by Spampinato et al. [31], each trial in the test set comes from a block with many trials in the training set. The results with and without bandpass filtering are shown in Tables 9 and 10 respectively and mirror the results in Tables 4 and 6 respectively. Note that with bandpass filtering, we obtain classification accuracies far higher than chance with the 1D CNN, while without bandpass filtering, we obtain near perfect classification accuracies, similar to those obtained in Tables 1–3.

Third, we reran the code released by Spampinato et al. [31] (an LSTM combined with a fully connected layer and a ReLU layer) on the data released by Spampinato et al. [31] but first applied various highpass filters with 14 Hz,

10 Hz, and 5 Hz cutoffs to the data. Recall, from Table 1, that we obtain a classification accuracy of 93% without such highpass filtering. With the highpass filtering, classification accuracy drops to 32.4% (14 Hz), 29.8% (10 Hz), and 29.7% (5 Hz).

### 3.8 Regression

In support of claim 2, Spampinato et al. [31, § 3.3 and § 4.2] report an analysis whereby they use the LSTM, combined with a fully connected layer and a ReLU layer, that was trained on EEG data as an encoder to produce a 128-element encoding vector for each image in their dataset. They then regress the 1,000-element output representation from a number of existing deep-learning object classifiers that have been pretrained on ImageNet to produce the same encoding vectors. When training this regressor, in some instances, they freeze the parameters of the existing deep-learning object classifiers, while in other instances they fine tune them while learning the regressor. They report a mean square error (MSE) between 0.62 and 7.63 on the test set depending on the particulars of the model and training regimen [31, Table 4]. They claim that this result supports the conclusion that this is the *the first human brain-driven automated visual classification method* and thus enables

TABLE 6

Application of the analysis from Table 3 to our new data collected with a block design on (left) image and (right) video stimuli, where our new data has not been preprocessed with bandpass filtering.

window	channels	LSTM	k-NN	SVM	MLP	1D CNN	window	channels	LSTM	k-NN	SVM	MLP	1D CNN
440 ms	96	63.1%	100.0%	100.0%	21.9%	85.9%	4000 ms	96	98.4%	97.9%	99.0%	77.6%	99.0%
200 ms	96	66.1%	99.9%	100.0%	35.8%	83.7%	2000 ms	96	94.8%	98.2%	99.5%	85.4%	99.0%
100 ms	96	71.8%	100.0%	100.0%	45.7%	n/a	1000 ms	96	96.9%	97.4%	99.0%	95.6%	99.0%
50 ms	96	70.2%	99.8%	100.0%	63.3%	n/a	500 ms	96	88.5%	96.4%	99.5%	98.7%	n/a
1 ms	96	59.7%	99.9%	99.8%	81.3%	n/a	1 ms	96	91.7%	97.4%	99.2%	98.7%	n/a
440 ms	64	70.6%	99.9%	100.0%	27.5%	76.4%	4000 ms	64	96.9%	96.9%	100.0%	68.2%	98.7%
200 ms	64	64.3%	100.0%	100.0%	34.1%	78.2%	2000 ms	64	95.8%	97.1%	100.0%	83.1%	99.0%
100 ms	64	68.1%	99.9%	100.0%	50.5%	n/a	1000 ms	64	94.3%	97.1%	100.0%	95.6%	98.4%
50 ms	64	70.9%	99.8%	100.0%	68.6%	n/a	500 ms	64	89.8%	96.6%	100.0%	99.0%	n/a
1 ms	64	58.1%	100.0%	99.5%	71.3%	n/a	1 ms	64	78.6%	97.9%	100.0%	97.9%	n/a
440 ms	32	64.1%	99.8%	100.0%	31.5%	74.7%	4000 ms	32	91.9%	96.9%	100.0%	75.0%	99.7%
200 ms	32	60.7%	99.7%	100.0%	43.9%	73.9%	2000 ms	32	77.1%	96.9%	100.0%	86.2%	97.9%
100 ms	32	63.1%	99.8%	100.0%	62.1%	n/a	1000 ms	32	85.7%	96.6%	100.0%	96.4%	98.7%
50 ms	32	66.4%	99.7%	100.0%	73.0%	n/a	500 ms	32	82.6%	96.1%	99.7%	99.2%	n/a
1 ms	32	45.6%	99.7%	99.0%	63.8%	n/a	1 ms	32	76.8%	97.9%	100.0%	96.9%	n/a
440 ms	24	48.4%	99.9%	100.0%	35.5%	73.3%	4000 ms	24	84.1%	96.9%	100.0%	83.3%	99.0%
200 ms	24	54.6%	99.7%	100.0%	51.5%	71.8%	2000 ms	24	83.9%	97.1%	100.0%	84.1%	99.0%
100 ms	24	59.4%	99.8%	100.0%	69.8%	n/a	1000 ms	24	69.3%	97.1%	100.0%	95.3%	98.7%
50 ms	24	71.1%	99.9%	100.0%	80.0%	n/a	500 ms	24	80.2%	96.9%	99.7%	97.9%	n/a
1 ms	24	50.7%	99.7%	98.7%	62.2%	n/a	1 ms	24	60.2%	95.6%	99.5%	95.8%	n/a
440 ms	16	51.5%	99.9%	100.0%	40.1%	70.2%	4000 ms	16	75.5%	96.9%	100.0%	69.8%	97.7%
200 ms	16	56.9%	99.8%	100.0%	55.8%	72.5%	2000 ms	16	74.7%	97.4%	100.0%	85.4%	95.6%
100 ms	16	63.2%	99.7%	100.0%	71.3%	n/a	1000 ms	16	63.5%	97.1%	100.0%	94.0%	98.4%
50 ms	16	63.8%	99.8%	100.0%	70.0%	n/a	500 ms	16	71.1%	97.7%	100.0%	96.9%	n/a
1 ms	16	45.3%	99.6%	98.8%	62.7%	n/a	1 ms	16	63.8%	97.7%	99.7%	91.1%	n/a
440 ms	8	31.8%	99.6%	99.9%	53.9%	71.5%	4000 ms	8	63.0%	97.9%	100.0%	80.2%	98.2%
200 ms	8	40.4%	99.5%	100.0%	63.4%	71.3%	2000 ms	8	62.0%	99.0%	99.7%	89.3%	99.2%
100 ms	8	54.2%	99.5%	99.8%	66.2%	n/a	1000 ms	8	78.9%	99.2%	100.0%	93.5%	98.4%
50 ms	8	61.2%	99.4%	99.3%	61.9%	n/a	500 ms	8	72.7%	99.0%	100.0%	96.9%	n/a
1 ms	8	46.0%	99.5%	98.7%	58.8%	n/a	1 ms	8	55.7%	98.7%	99.5%	90.4%	n/a

TABLE 7

Application of the analysis from Table 1 to our new data collected with a rapid-event design on (left) image and (right) video stimuli, where our new data has not been preprocessed with bandpass filtering.

LSTM	k-NN	SVM	MLP	1D CNN	LSTM	k-NN	SVM	MLP	1D CNN
0.7%	1.4%	2.7%	1.5%	2.1%	10.2%	8.3%	7.3%	9.6%	10.7%

automated visual classification in a “brain-based visual object manifold” [31, § 5 p. 6816].

Note that Spampinato et al. [31] use the same LSTM combined with a fully connected layer and a ReLU layer both as a classifier and as an encoder. During training as a classifier, the output of the last layer of the classifier, namely the ReLU, is trained to match the class label. Thus using such a trained classifier as an encoder would tend to encode EEG data in a representation that is close to class labels. Crucially, the output of the classifier taken as an encoder contains mostly, if not exclusively, class information and little or no reflection of other non-class-related visual information. Further, since the output of their classifier is a 128-element vector, since they have 40 classes, and since they train with a cross-entropy loss that combines log softmax with a negative log likelihood loss, the classifier tends to produce an output representation whose first 40 elements contain an approximately one-hot-encoded representation of the class label, leaving the remaining elements at zero. Indeed, we observe this property of the encodings produced by the code released by Spampinato et al. [31] on the data released by Spampinato et al. [31] (Fig. 2). Note that the diagonal nature of Fig. 2 reflects an approximate one-hot class encoding. Any use of a classifier trained in this fashion as an encoder would have this property. Spampinato et al. [31, § 3.3, § 4.2, and § 4.4] use such an encoder to train an

object classifier with EEG data, Palazzo et al. [20], Kavasidis et al. [15], and Tirupattur et al. [35] use such an encoder to train a variational autoencoder (VAE) [16] or a generative adversarial network (GAN) [10] to produce images of human perception and thought, and Palazzo et al. [21] use such an encoder to produce saliency maps, EEG activation maps, and to measure association between EEG activity and layers in an object detector. Thus all this work is essentially driven by encodings of class information that lack any visual information or any representation of brain processing.

We ask whether there is merit in the regression algorithm proposed by Spampinato et al. [31] to create a novel object classifier driven by brain signals. We analyze their algorithm under the assumption that it is applied to EEG data that supports classification of visually perceived objects and does not suffer from contamination. Under this assumption, the EEG response of two images of the same class would be closer than for two images of different classes. An encoder like the one employed by Spampinato et al. [31] would produce encodings that are more similar for images of the same class than images of different classes. (For their actual encoder, Fig. 2 shows that they are indeed little more than class encodings). Moreover, deep-learning object classifiers presumably produce closer representations for images in the same object class than for images of different classes. After all, that is what object classifiers do. Thus all the

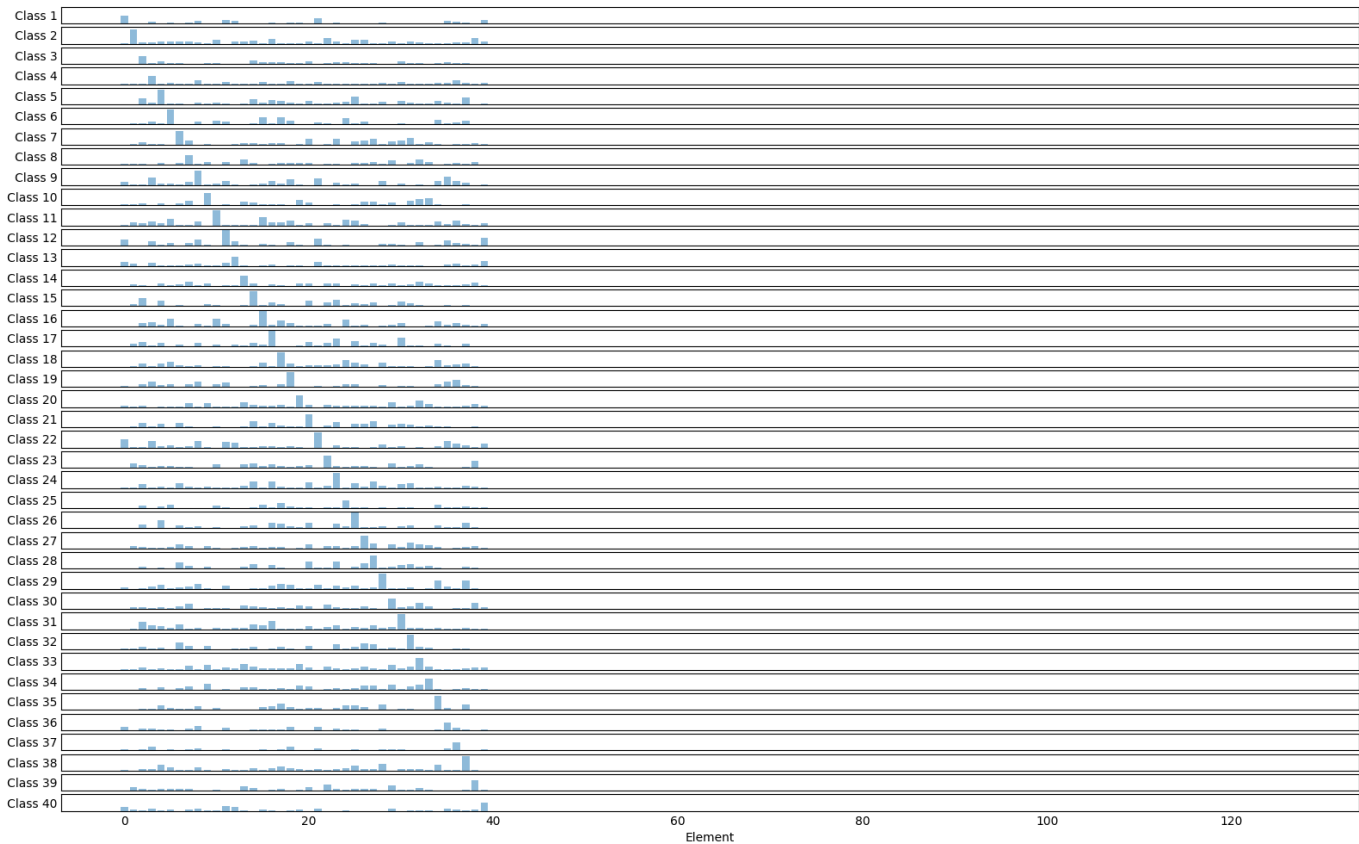


Fig. 2. Encodings of the measured EEG response to each of the 40 ImageNet classes, as produced by the LSTM-based encoder of Spampinato et al. [31] on the EEG data released by Spampinato et al. [31], averaged across all six subjects and all 50 images per class.

regressor does is preserve the property that two images of the same class regress to closer representations than two images of different classes. In other words, all the regressor does is map a 1,000-dimension representation of class to a 128-dimension representation of class. It should not matter whether the actual target representation is a reflection of brain processing or not.

We asked whether the putative success of this regression analysis depended on a representation derived from neuroimaging. To this end, we generated a random codebook with random codewords that simulate the EEG response of all six subjects to all 2,000 image stimuli. This was done with the following procedure. We first generated 40 random codewords, one for each class, by uniformly sampling elements i.i.d in  $[0, 2]$ . We then generated  $50 \times 6 = 300$  random codewords for each class, one for each subject and image, by adding univariate Gaussian noise with  $\sigma^2 = 4$  i.i.d. to the elements of the class codewords, and clipped the elements to be nonnegative. This generated a codebook of 12,000 random codewords for each simulated subject response that has the property that encodings for images in the same class are closer than entries for images in different classes. These codewords carry no brain-inspired meaning whatsoever. Like Spampinato et al. [31], we then averaged the codewords across subject for each image. We then applied the PyTorch VGG-16 [24] pretrained on ImageNet, without any fine tuning, to each of the images in the Spampinato et al. [31] dataset. Finally, we trained a linear regressor with MSE

loss and L2 regularization from the output of VGG-16 on each image to the average random codeword for that image on the training set for the first split provided by Spampinato et al. [31]. We then measured an average MSE of 0.55 on the validation and test sets of that split. The fact that it is possible to regress the output of an off-the-shelf pretrained object classifier to random class encodings as well as one can regress that output to class encodings derived from an EEG encoder demonstrates that the ability to do so does not depend on anything other than class information in the source and target representations.

### 3.9 Transfer learning

In further support of claim 2, Spampinato et al. [31, § 4.4] report an analysis that purports to demonstrate that the learned combination of regressor and object classifier generalizes to other datasets with disjoint sets of classes. To this end, they first apply VGG-16, pretrained on ImageNet, to a subset of the Caltech 101 [9] dataset with 30 classes, not fine tuned, to produce a 1,000-element representation of each image. They then map this with their regressor trained as described above to 128-element encodings. Finally, they train and test an SVM classifier on the resulting encodings. They compare this with an SVM classifier trained and tested on the 1,000-element outputs from pretrained deep-learning object classifiers that have not been mapped with their regressor and achieve comparable performance (92.6% on the

TABLE 8  
Reanalysis of the data released by Spampinato et al. [31] with classification accuracy averaged over leave-one-subject-out round-robin cross validation instead of the provided splits.

window	channels	LSTM	k-NN	SVM	MLP	1D CNN
440 ms	128	2.7%	3.4%	3.4%	3.4%	3.1%
200 ms	128	2.4%	3.5%	3.3%	3.5%	3.1%
100 ms	128	3.0%	3.4%	3.5%	2.6%	n/a
50 ms	128	2.9%	3.3%	3.0%	2.4%	n/a
1 ms	128	3.0%	2.2%	3.1%	3.0%	n/a
440 ms	96	3.3%	3.0%	3.4%	2.6%	3.3%
200 ms	96	2.3%	3.0%	3.3%	3.6%	4.0%
100 ms	96	2.8%	2.6%	3.1%	3.5%	n/a
50 ms	96	2.9%	2.6%	3.2%	2.5%	n/a
1 ms	96	2.7%	2.4%	3.2%	3.2%	n/a
440 ms	64	2.6%	2.3%	3.4%	3.6%	3.6%
200 ms	64	3.2%	2.2%	3.0%	2.7%	3.2%
100 ms	64	2.7%	2.2%	3.2%	3.2%	n/a
50 ms	64	2.6%	2.0%	2.9%	3.2%	n/a
1 ms	64	2.7%	2.4%	3.0%	3.0%	n/a
440 ms	32	2.6%	1.9%	3.7%	2.6%	3.6%
200 ms	32	3.0%	1.8%	3.9%	3.4%	2.7%
100 ms	32	3.4%	1.9%	3.8%	2.6%	n/a
50 ms	32	2.6%	2.1%	4.2%	3.2%	n/a
1 ms	32	1.8%	2.3%	2.8%	3.2%	n/a
440 ms	24	2.3%	2.3%	3.7%	2.6%	2.9%
200 ms	24	2.5%	2.5%	3.6%	2.7%	2.7%
100 ms	24	3.1%	2.4%	3.6%	2.4%	n/a
50 ms	24	3.0%	2.8%	3.6%	2.5%	n/a
1 ms	24	2.9%	3.0%	3.0%	2.5%	n/a
440 ms	16	2.0%	2.1%	2.5%	2.7%	2.8%
200 ms	16	1.9%	2.1%	2.7%	2.7%	2.7%
100 ms	16	2.7%	2.2%	2.3%	2.6%	n/a
50 ms	16	2.6%	2.4%	2.9%	2.5%	n/a
1 ms	16	3.1%	2.6%	3.2%	2.8%	n/a
440 ms	8	2.1%	2.3%	2.8%	3.0%	2.9%
200 ms	8	2.8%	2.3%	2.5%	2.8%	2.4%
100 ms	8	2.6%	2.3%	2.5%	3.1%	n/a
50 ms	8	1.9%	2.4%	2.8%	2.8%	n/a
1 ms	8	2.8%	2.2%	3.0%	2.7%	n/a

1,000-element output of GoogleNet and 89.7% on the 128-element encodings regressed from GoogleNet). They claim that their approach enables *automated visual classification in a “brain-based visual object manifold”* and *show[s] competitive performance, especially as concerns learning EEG representation of object classes* [31, § 5 p. 6816].

We conjecture that the putative success of this transfer-learning analysis is not surprising and demonstrates nothing about the quality of the representation nor whether it reflects brain processing. As discussed above, the deep-learning object classifiers produce closer output representations for images in the same object class than for images of different classes. Further, as discussed above, all the regressor does is preserve the property that two images of the same class regress to closer encodings than two images of different classes. The choice of regressor or regressed representation should have no impact on the SVM classifier so long as these properties hold.

We thus asked whether the putative success of this transfer-learning analysis depended on a representation derived from neuroimaging. To this end, we used VGG-16, pretrained on ImageNet without any fine tuning, to map the images in Caltech 101 to 1,000-element encodings and applied the regressor that we trained on random representations to map these 1000-element encodings to 128-element encodings. This composite mapping exhibited the above

properties. This, again, generated a codebook of random codewords for each image in this subset of Caltech 101 that has the property that entries for images in the same class are closer than entries for images in different classes. As before, the codewords carry no brain-inspired meaning. We split our subset of Caltech 101 into disjoint training and test sets, trained a linear SVM on the training set, and achieved an accuracy of 95.9% on the test set when classified on the 128-element encodings regressed from VGG-16 as compared with 94.9% on the test set when classified on the 1,000-element output of VGG-16.

## 4 RECONCILING DISCREPANCIES

A number of papers, *e.g.*, Spampinato et al. [30, Figs. 1 and 2(c)], Palazzo et al. [20, Figs. 1 and 2], and Kavasidis et al. [15, Figs. 2, 3, and 4], use an encoder that appears to be similar or identical to that reported in Spampinato et al. [31, Figs. 2 and 3(c)].<sup>7</sup> A number of papers [8, 15, 20, 21] use the dataset reported in Spampinato et al. [31].<sup>8</sup> Spampinato et al. [31] have released the code<sup>1</sup> for their encoder as well as their data<sup>2</sup>. They have released their data in two formats, Python and Matlab. We have observed a number of discrepancies between the different published accounts, between the different released variants of the data, and between the published accounts and the released code and data. We discuss here how we reconciled such for the purposes of the experiments and analyses reported here. We do this solely to document precisely what we have done. We do not believe that anything substantive turns on these issues, except for the issue of filtering, whether or not the DC and VLF components are removed from the EEG data. In this case, we perform all analyses twice, with and without such removal.

### 4.1 Filtering

Spampinato et al. [30, § 3.1 p. 7] state:

*A notch filter (49–51 Hz) and a second-order band-pass Butterworth filter (low cut-off frequency 14 Hz, high cut-off frequency 71 Hz) were set up so that the recorded signal included the Beta (15–31 Hz) and Gamma (32–70 Hz) bands, as they convey information about the cognitive processes involved in the visual perception [15].*

Spampinato et al. [31, § 3.1 p. 6812] state:

*A notch filter (49–51 Hz) and a second-order band-pass Butterworth filter (low cut-off frequency 14 Hz, high cut-off frequency 71 Hz) were set up so that the recorded signal included the Beta (15–31 Hz) and Gamma (32–70 Hz) bands, as they convey information about the cognitive processes involved in the visual perception [15].*

Palazzo et al. [20, §3.1 p. 3412] state:

<sup>7</sup>Palazzo et al. [20] and Tirupattur et al. [35] appear to employ related but somewhat different encoders. We do not comment on these here since we do not have access to this code.

<sup>8</sup>An earlier but similar dataset was reported in Spampinato et al. [30]. Tirupattur et al. [35] use a different dataset reported by Kumar et al. [17]. We do not comment on these here since we do not have access to these datasets.

TABLE 9

Reanalysis of our new data collected with a rapid-event design on (left) image and (right) video stimuli with incorrect block-level labels, where our new data has been preprocessed with bandpass filtering.

window	channels	LSTM	<i>k</i> -NN	SVM	MLP	1D CNN	window	channels	LSTM	<i>k</i> -NN	SVM	MLP	1D CNN
440 ms	96	9.2%	2.3%	2.7%	3.1%	47.7%	4000 ms	96	19.8%	7.3%	8.3%	6.5%	72.9%
200 ms	96	8.8%	2.3%	2.6%	3.2%	38.3%	2000 ms	96	18.8%	8.1%	8.9%	7.3%	74.2%
100 ms	96	6.9%	2.8%	3.5%	2.5%	n/a	1000 ms	96	20.3%	8.1%	7.8%	8.1%	70.1%
50 ms	96	6.3%	2.9%	3.3%	3.2%	n/a	500 ms	96	15.9%	9.4%	9.4%	6.5%	n/a
1 ms	96	3.1%	2.5%	2.5%	2.6%	n/a	1 ms	96	9.6%	9.9%	8.1%	9.4%	n/a
440 ms	64	6.3%	2.4%	2.0%	2.4%	34.4%	4000 ms	64	16.9%	8.3%	6.3%	6.8%	66.7%
200 ms	64	4.1%	2.6%	2.3%	2.9%	28.3%	2000 ms	64	13.0%	8.1%	9.1%	8.3%	66.1%
100 ms	64	4.0%	2.0%	2.5%	2.1%	n/a	1000 ms	64	15.9%	7.3%	7.3%	7.8%	60.2%
50 ms	64	3.9%	2.1%	2.5%	2.8%	n/a	500 ms	64	13.5%	8.6%	8.3%	8.3%	n/a
1 ms	64	3.1%	2.2%	3.0%	3.8%	n/a	1 ms	64	10.9%	9.1%	9.6%	8.9%	n/a
440 ms	32	3.6%	2.1%	2.0%	2.3%	17.7%	4000 ms	32	11.5%	6.3%	6.3%	7.6%	42.7%
200 ms	32	2.7%	2.7%	2.5%	2.4%	13.8%	2000 ms	32	9.9%	9.4%	8.9%	7.3%	44.5%
100 ms	32	2.1%	2.5%	2.6%	2.4%	n/a	1000 ms	32	8.6%	9.9%	10.2%	12.2%	35.4%
50 ms	32	2.4%	2.2%	2.5%	3.3%	n/a	500 ms	32	14.1%	9.1%	7.3%	8.1%	n/a
1 ms	32	3.5%	3.1%	2.4%	3.2%	n/a	1 ms	32	10.4%	10.4%	10.2%	9.6%	n/a
440 ms	24	2.9%	1.7%	2.9%	2.8%	15.0%	4000 ms	24	18.0%	4.2%	6.3%	7.0%	46.1%
200 ms	24	3.8%	2.4%	2.5%	1.8%	15.4%	2000 ms	24	12.0%	7.8%	9.1%	7.3%	32.0%
100 ms	24	4.0%	2.1%	2.8%	2.6%	n/a	1000 ms	24	12.8%	8.9%	10.2%	7.6%	44.3%
50 ms	24	2.6%	2.1%	2.9%	2.9%	n/a	500 ms	24	7.6%	7.8%	10.2%	5.7%	n/a
1 ms	24	3.6%	2.7%	2.5%	3.0%	n/a	1 ms	24	10.2%	9.1%	5.7%	7.8%	n/a
440 ms	16	2.5%	1.7%	2.9%	2.7%	12.8%	4000 ms	16	15.6%	7.3%	4.2%	7.0%	49.5%
200 ms	16	3.3%	2.4%	3.0%	2.7%	10.0%	2000 ms	16	14.6%	9.1%	7.3%	9.9%	37.8%
100 ms	16	2.7%	2.3%	2.2%	2.0%	n/a	1000 ms	16	10.7%	8.6%	10.2%	11.2%	36.2%
50 ms	16	2.5%	2.9%	3.3%	2.4%	n/a	500 ms	16	13.0%	6.5%	8.3%	8.1%	n/a
1 ms	16	3.6%	3.0%	2.3%	2.2%	n/a	1 ms	16	7.8%	9.6%	7.3%	7.8%	n/a
440 ms	8	2.1%	1.6%	2.5%	2.7%	6.9%	4000 ms	8	10.2%	9.4%	8.3%	8.6%	28.1%
200 ms	8	3.0%	2.0%	2.7%	2.4%	9.7%	2000 ms	8	13.3%	8.9%	8.1%	7.6%	40.3%
100 ms	8	3.4%	1.8%	3.1%	2.3%	n/a	1000 ms	8	9.6%	8.3%	9.9%	11.5%	21.4%
50 ms	8	2.4%	2.5%	2.4%	2.4%	n/a	500 ms	8	9.9%	8.1%	7.8%	7.3%	n/a
1 ms	8	2.7%	3.1%	2.1%	2.4%	n/a	1 ms	8	7.6%	8.9%	9.1%	10.2%	n/a

TABLE 10

Reanalysis of our new data collected with a rapid-event design on (left) image and (right) video stimuli with incorrect block-level labels, where our new data has not been preprocessed with bandpass filtering.

window	channels	LSTM	<i>k</i> -NN	SVM	MLP	1D CNN	window	channels	LSTM	<i>k</i> -NN	SVM	MLP	1D CNN
440 ms	96	76.7%	99.8%	100.0%	37.8%	95.4%	4000 ms	96	93.5%	97.9%	100.0%	78.4%	100.0%
200 ms	96	74.3%	99.8%	100.0%	53.5%	98.6%	2000 ms	96	95.3%	98.7%	100.0%	86.7%	99.7%
100 ms	96	78.8%	99.8%	100.0%	65.0%	n/a	1000 ms	96	98.4%	98.4%	100.0%	89.6%	99.7%
50 ms	96	80.7%	99.9%	100.0%	83.9%	n/a	500 ms	96	96.6%	98.2%	100.0%	98.7%	n/a
1 ms	96	58.4%	99.9%	100.0%	98.8%	n/a	1 ms	96	88.5%	97.1%	100.0%	99.0%	n/a
440 ms	64	66.3%	99.8%	100.0%	29.9%	96.3%	4000 ms	64	90.9%	97.9%	100.0%	74.0%	98.7%
200 ms	64	67.6%	99.8%	100.0%	36.1%	96.3%	2000 ms	64	76.3%	99.0%	99.5%	78.1%	98.4%
100 ms	64	72.9%	99.9%	100.0%	61.7%	n/a	1000 ms	64	89.8%	98.2%	99.7%	85.9%	99.0%
50 ms	64	75.0%	99.8%	100.0%	89.5%	n/a	500 ms	64	91.9%	98.2%	99.7%	96.4%	n/a
1 ms	64	96.2.1%	99.9%	100.0%	93.0%	n/a	1 ms	64	82.3%	97.9%	99.7%	97.4%	n/a
440 ms	32	51.4%	99.3%	100.0%	31.3%	84.9%	4000 ms	32	80.2%	96.9%	99.0%	58.3%	94.8%
200 ms	32	62.2%	99.5%	100.0%	46.7%	82.4%	2000 ms	32	73.7%	96.6%	99.0%	81.5%	95.8%
100 ms	32	65.6%	99.4%	100.0%	73.5%	n/a	1000 ms	32	81.5%	96.6%	99.5%	88.5%	96.4%
50 ms	32	64.8%	99.5%	100.0%	86.6%	n/a	500 ms	32	76.3%	96.9%	99.5%	93.0%	n/a
1 ms	32	49.0%	99.2%	97.9%	71.2%	n/a	1 ms	32	66.4%	96.6%	99.2%	89.3%	n/a
440 ms	24	50.7%	99.4%	100.0%	36.1%	81.4%	4000 ms	24	84.4%	95.8%	100.0%	64.8%	95.3%
200 ms	24	60.0%	99.4%	100.0%	60.0%	80.8%	2000 ms	24	84.4%	96.4%	100.0%	78.4%	94.0%
100 ms	24	55.3%	99.4%	100.0%	76.7%	n/a	1000 ms	24	72.9%	95.1%	99.7%	83.6%	90.6%
50 ms	24	63.3%	99.3%	99.9%	82.9%	n/a	500 ms	24	84.6%	96.6%	100.0%	95.3%	n/a
1 ms	24	50.9%	99.3%	97.8%	70.5%	n/a	1 ms	24	60.9%	97.9%	99.2%	88.5%	n/a
440 ms	16	46.9%	99.3%	100.0%	45.0%	80.5%	4000 ms	16	68.8%	93.8%	99.0%	66.9%	91.4%
200 ms	16	53.6%	99.2%	100.0%	66.0%	76.5%	2000 ms	16	73.7%	93.5%	99.7%	83.1%	89.1%
100 ms	16	63.9%	99.0%	100.0%	80.9%	n/a	1000 ms	16	66.9%	93.5%	98.2%	91.7%	90.4%
50 ms	16	63.1%	99.0%	99.8%	84.6%	n/a	500 ms	16	68.0%	93.2%	99.0%	88.8%	n/a
1 ms	16	43.0%	98.8%	96.8%	64.1%	n/a	1 ms	16	54.4%	94.5%	96.1%	84.9%	n/a
440 ms	8	37.8%	98.4%	99.4%	60.3%	69.0%	4000 ms	8	68.8%	94.8%	99.0%	75.5%	90.9%
200 ms	8	41.4%	98.5%	99.6%	71.2%	70.9%	2000 ms	8	57.3%	92.4%	97.9%	81.3%	87.5%
100 ms	8	52.6%	98.5%	99.2%	75.5%	n/a	1000 ms	8	58.9%	93.0%	98.2%	89.8%	88.8%
50 ms	8	54.3%	98.1%	98.8%	75.8%	n/a	500 ms	8	63.5%	93.5%	98.2%	89.6%	n/a
1 ms	8	44.2%	98.3%	95.0%	55.5%	n/a	1 ms	8	52.1%	93.2%	92.4%	80.7%	n/a

*The acquired EEG signals were filtered in run-time (i.e., during the acquisition phase) by the integrated hardware notch filter (49–51 Hz) and a second order Butterworth (band-pass) filter with frequency boundaries 14–70 Hz. This frequency range contains the necessary bands (Alpha, Beta and Gamma) that are most meaningful during the visual recognition task [17].*

Later publications [15, 21, 35] do not discuss filtering.

A spectral analysis (Fig. 3) of both the Python and Matlab format data released by Spampinato et al. [31] suggests that neither have been filtered by any notch filter nor any band-pass filter. The Python and Matlab format data differ greatly, and have somewhat different spectra. The code originally released by Spampinato et al. [31] does not contain any notch filtering or any bandpass filtering, but does contain z-scoring. We asked the authors to clarify [14]. Email reply from Spampinato [26] stated:

We did very little pre-processing (notch filtering and normalization) on the data.

We provided [32] an early draft of this manuscript to the authors of Spampinato et al. [31]. That draft pointed out the spectral analysis. Email response from Palazzo [19] stated:

Our released dataset is not preprocessed but raw, directly coming from the EEG device that does not allow us to perform the erroneous filtering you are suggesting.

In further response, email from Spampinato [27] stated:

As we said to you in our previous email exchanges, we did not perform any pre-processing except notch filtering and normalization (there is a misprint in our original paper, despite in the work webpage we haven't reported that filtering) and this processing was done during models' training on the raw EEG data (the one available online).

In response to further requests for clarification, email from Spampinato [28] stated:

all the results reported in the paper are obtained with the code [http://perceive.dieei.unict.it/files/cvpr\\_2017\\_eeg\\_encoder.py](http://perceive.dieei.unict.it/files/cvpr_2017_eeg_encoder.py) (with the exception that we performed notch filtering with an additional code that it is not online but we can send to you) on the .pth data at <https://cloud.perceive.dieei.unict.it/index.php/s/XFF23FHapphsTut/download>. Results may be slightly different because different hyperparameters and epochs.

We haven't done any analysis on the matlab file (I suggest you not to use it). We also noticed that that data is slightly different (despite the dynamic is the same) from the python version (but we only opened the raw

file with EEGLab and export it as mat file).

No filtering was applied at the acquisition time and before generating the python data available online.

Further email from Spampinato [29] stated:

attached you can find the revised version of the [http://perceive.dieei.unict.it/files/cvpr\\_2017\\_eeg\\_encoder.py](http://perceive.dieei.unict.it/files/cvpr_2017_eeg_encoder.py) which includes notch filtering and [0–71]hz passband filtering that you can use for your tests. This newest code is written in PyTorch 0.4 (the online version is 0.3) which should be more efficient.

We take this all to imply that no filtering was applied during acquisition, no filtering was applied prior to production of either the Python or Matlab format released data, the analyses reported in Spampinato et al. [31] were performed using the released code version 0.3 which did not perform any filtering, and any filtering code was added subsequent to our contact with Spampinato et al. [31].

Examination of version 0.4 of the code provided to us indicates that the data was first z-scored, then notch filtered (47–53 Hz), and then lowpass filtered (71 Hz), all on a segment-by-segment basis. This is unconventional in five ways. First, z-scoring would normally be done after filtering, not before. Second, z-scoring would normally be done after segmentation, not before. Third, filtering would normally be done before segmentation, not after. Fourth, the notch filter employed a different notch band than previously reported. Fifth, the data was lowpass filtered rather than bandpass filtered. All analyses reported here were performed with the released (version 0.3) code, modified as discussed below, on the Python format data, unmodified, except as discussed below and in the text.

## 4.2 Quantization

Spampinato et al. [31, § 3.1 p. 6813] state:

*Data value distribution was centered around zero, thus non-linear quantization was applied.*

Palazzo et al. [20, § 3.1 p. 3413] similarly state:

*The histogram of the acquired signals over the different values presented with a high density near the zero value and a much lower density at the extremities. In order to reduce input space sparsity, non-uniform quantization was applied for data compression.*

As the released code contains no indication of such, we have no way of knowing sufficient details of how to replicate this quantization on our data. We further have no way of knowing if the released Python and/or Matlab data reflects this quantization or not. Thus we do not perform any quantization on either the released data or our new data as part of any analyses reported here.

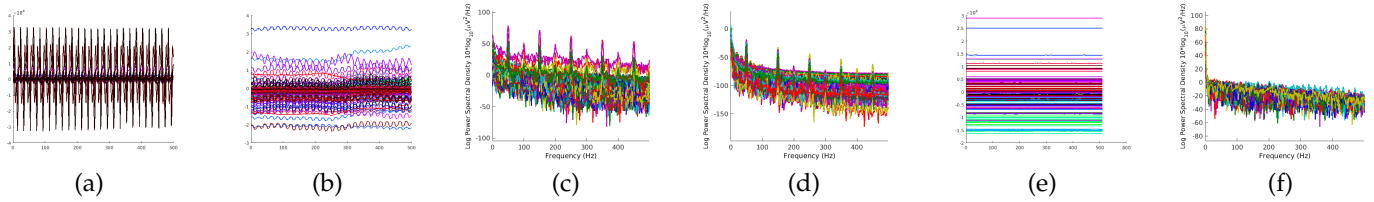


Fig. 3. Waveforms of the EEG data for the ImageNet image stimulus `n02124075_12647`, as provided by Spampinato et al. [31] for Subject 1, in (a) Python format and (b) Matlab format. Corresponding spectra of the (c) Python format and (d) Matlab format data. (e) Waveforms and (f) spectra for the same stimulus in our raw unfiltered data collected with a block design.

### 4.3 Trials considered

Spampinato et al. [31] nominally collected 50 trials for each of 40 stimuli and 6 subjects for a total of 12,000 trials. However, Palazzo et al. [20, § 3.1 p. 3413] state:

*Given that the systems involved are not real-time (Operating system process scheduler, DAQ hardware etc. . .), variable length EEG sequences were dealt with by discarding those with less than 480 samples. Data sequences whose length was between 480 and 500 samples w[h]ere padded with zeros until reaching 500 samples. Sequences longer than 500 samples were tail trimmed. [...] 534 samples did not satisfy the minimum data length criteria described above, resulting in 11,466 valid samples.*

Kavasidis et al. [15, § 3.1 p. 1811] further state:

*After the EEG data acquisition, we obtained 11,466 128-channel EEG sequences (536 recordings were discarded because they were too short or too altered to be included in the experiment). [20, § 3.1 p. 3413]*

The released data in Python format contains 11,965 trials which is a superset of the released data in Matlab format that contains 11,466 trials. Further, the Python format data differs from the Matlab format data. We have no way of knowing why the data differs, why the Python format data contains 11,965 trials, and whether the 11,466 trials in the Matlab format data correspond to the 11,466 trials reported above. Nonetheless, we take 536 *vs.* 534 to be a typo and use the Python format data, but only those 11,466 trials that appear in the Matlab format data. The 499 trials thus discarded come from Subject 2.

### 4.4 Trial window

The published papers indicate that samples 40–480 were used. Spampinato et al. [31, § 3.1 p. 6813] state:

*From each recorded EEG sequence, the first 40 samples (40 ms) for each image were discarded in order to exclude any possible interference from the previously shown image (i.e., to permit the stimulus to propagate from the retina through the optical tract to the primary visual cortex [8]). The following 440 samples (440 ms) were used for the experiments.*

Palazzo et al. [20, § 3.1 p. 3413] further state:

*From each recorded EEG sequence, the first 40 samples were discarded in order to minimize any possible interference from the previously shown image (i.e., to give the necessary time for the stimulus to clear its way through the optical tract [9]). The following 440 samples (440 ms) were used for the experiments.*

Palazzo et al. [21, §7.1 p. 7] further state:

*The exact duration of each signal may vary, so we discard the first 40 samples (40 ms) to reduce interferences from the previous image and then cut the signal to a common length of 440 samples (to account for signals with  $L < 500$ ), when supposedly all image-related visual and cognitive processes will have been completed.*

The released code, however, uses samples 20–450 (i.e., a sequence of length 430), lacks zero padding and tail trimming, and discards sequences shorter than 450 samples or longer than 600 samples. No trials are shorter than 480 samples so none are discarded for this reason and none require zero padding. The released code, however, discards 25 trials beyond the 534 mentioned above for being longer than 600 samples. We have no way of knowing what was actually done to obtain the results in Spampinato et al. [31], Palazzo et al. [20], Kavasidis et al. [15], and Palazzo et al. [21]. Here, we modified the released code to not discard (the 25) trials longer than 600 samples and to use samples 40–480 from each trial instead of 20–450.

### 4.5 The encoder model

When describing the encoder model ([30, Figs. 1 and 2(c)], [20, Figs. 1 and 2], and [15, Figs. 2, 3, and 4]), Spampinato et al. [30, § 3.2 p. 9] state:

*an additional output layer (linear combinations of input, followed by ReLU nonlinearity) is added after the LSTM*

Spampinato et al. [31, § 3.2 p. 6813] similarly state:

*an additional output layer (linear combinations of input, followed by ReLU nonlinearity) is added after the LSTM*

Palazzo et al. [20, § 3.2 p. 3414] similarly state:

*the final output state of the LSTM goes into a fully-connected layer with ReLU non-linearity.*

Kavasidis et al. [15, § 3.2 p. 1811] similarly state:

*The first processing module of our approach consists of an encoder, which receives as input an EEG time series and provides as output a more compact and class-discriminative feature vector. In [26] we tested several encoder models and the most performing one is shown in Fig. 4. It consists of a standard LSTM layer followed by a nonlinear layer. An input EEG sequence is fed into the LSTM layer, whose output at the final time step goes into a fully-connected layer with a ReLU activation function. This simple architecture when stacked with a 40-way softmax layer yielded good performance—over 80% classification accuracy.*

However, the released code omits the ReLU layer. We modified the released code to add the ReLU layer for the analyses reported here.

#### 4.6 The classifier

Spampinato et al. [30, Fig. 1] and Spampinato et al. [31, Fig. 2] report training the encoder by attaching a classifier to its output and training against known labels. Spampinato et al. [30, § 3.2 p. 8] state:

*The encoder network is trained by adding, at its output, a classification module (in all our experiments, it will be a softmax layer), and using gradient descent to learn the whole model/s parameters end-to-end.*

Spampinato et al. [30, § 3.3 p. 10] state:

*modified it by replacing the softmax classification layer with a regression layer*

Spampinato et al. [30, § 4.3 p. 14] state:

*Our automated visual classifier consists of the combination of the CNN-based feature regressor achieving the lowest MSE (GoogleNet features with k-NN regressor, trained on average features) with the softmax classifier trained during EEG manifold learning.*

Spampinato et al. [31, § 3.2 p. 6813] state:

*The encoder network is trained by adding, at its output, a classification module (in all our experiments, it will be a softmax layer), and using gradient descent to learn the whole model's parameters end-to-end.*

Spampinato et al. [31, § 3.3 p. 6814] state:

*modified it by replacing the softmax classification layer with a regression layer*

Spampinato et al. [31, § 3.3 p. 6814] state:

*The resulting CNN-based regressor is able to extract brain-learned features from any input image for further classification by the softmax layer trained during EEG feature learning.*

Spampinato et al. [31, § 4.3 p. 6816] state:

*and then classifies feature vectors using the softmax classifier trained during EEG manifold learning.*

Palazzo et al. [20, § 3.2 p. 3414] state:

*We append a softmax classification layer and perform gradient descent optimization (supervised by the class of the image shown when the input signal had been recorded) to train the encoder and the classifier end-to-end.*

Kavasidis et al. [15, § 3.2 p. 1811] state:

*This simple architecture when stacked with a 40-way softmax layer yielded good performance — over 80% classification accuracy.*

Kavasidis et al. [15, § 4.3 p. 1815] state:

*with the softmax layer changed for a 40-class classification task.*

Tirupattur et al. [35, § 4.3 p. 954] state:

*We use ReLU activation for all the layers in our network and Softmax for the final classification layer.*

Palazzo et al. [21, § 7.2 p. 8] state:

*Once training is completed, we use the trained EEG and image encoders as feature extractors in the joint embedding space, followed by a softmax layer, for both image and EEG classification.*

Palazzo et al. [21, § 7.2 p. 8] state:

*Both our model and pre-trained visual encoders are used as feature extractors followed by a softmax layer*

The released code appears to use PyTorch `torch.nn.functional.cross_entropy`, which internally uses `torch.nn.functional.log_softmax`. This is odd for two reasons. First, this has no parameters and does not require any training. Second, training a 40-way classifier this way, appended to an encoder, with an implicit one-hot representation of class labels, will tend to train the encoder to produce 128-element EEG encodings where all but the first 40 elements are zero (Fig. 2). Indeed, we have observed this behavior with the released code. We have no way of knowing what was actually intended and used to generate the reported results. Here, like the released code, we train the encoders with the same cross-entropy loss, which internally contains a log softmax operation, but use the output of the encoder, prior to any softmax operation, for classification. (Note that had the output of the softmax layer been taken as the EEG encodings, they would have been one-hot.)

## 5 DISCUSSION

The analyses in § 3.3 demonstrate that the results reported by Spampinato et al. [31] do not depend on the temporal structure of the EEG signal. The analyses in § 3.5 demonstrate that the results reported by Spampinato et al. [31] crucially depend on a block design and cannot be replicated with a rapid-event design. However, the block design of Spampinato et al. [31], together with their training/test-set splits, is such that every trial in each test set comes from a block that has many trials in the corresponding training set. The first analysis in § 3.7 shows that if one adopts splits that separate trials from a block so that the test sets never contain trials from blocks that have any trials in the corresponding training sets, classification accuracy drops to chance. This strongly suggests that the high classification accuracy obtained by Spampinato et al. [31] crucially depends on such contamination, which constituted surreptitious training on the test set. This is further corroborated by the second analysis in § 3.7 that shows that one can obtain near perfect classification accuracy with an experiment design where labels vary only by block but where the class of the stimuli within the block are uncorrelated with the labels. If the methods of Spampinato et al. [31] were indeed classifying brain activity due to perception of the class of the stimuli, one would expect to obtain chance performance with this analysis. The fact that near perfect performance was obtained strongly suggests that these methods are indeed classifying the long-term static brain activity that persists during a block that is uncorrelated with the perceptual activity. Finally, the third analysis in § 3.7 shows that this finding is exacerbated by the presence of DC and VLF components of the recorded EEG signal that are present due to the omission of bandpass filtering. We propose that all future classification experiments performed on EEG data employ a design that controls for such contamination. Since the data released by Spampinato et al. [31] irreparably suffers from this contamination, it renders this dataset unsuitable for its intended purpose of decoding perceptual and conceptual processing and further

invalidates all subsequent analyses and claims that use this data for those purposes [8, 15, 20, 21].

### 5.1 Consequences of flawed filtering

While Spampinato et al. [31] and two related papers [20, 30] suggest that the reported results were obtained with a process that included notch and bandpass filtering, subsequent analysis and communication with the authors now suggest that this was not the case (§ 4.1). This analysis and communication with the authors has led them to modify their code (§ 4.1). This is important for two reasons. First, the modifications that they made do not address the issue at hand. The added lowpass (71 Hz) filter does not address the data contamination problem resulting from the block design that leads to surreptitious training on the test set. Further, it preserves the DC and VLF components that exacerbate that problem. It is those components, not the HF components, that need to be removed. Even doing this would only address the exacerbation. It would not address the root cause which is the block design. Second, the fact that the authors omitted the bandpass filter exacerbated the issue, leading to egregious overestimation of the classification accuracy. This has led to their results and data receiving considerable attention and enthusiasm, possibly contributing to the sheer number of papers that use this dataset and/or pursue similar approaches. Had the stated filtering been performed, perhaps the resulting more modest (but still invalid) results would have tempered the rapid proliferation of follow-up work that also suffers from similar methodological shortcomings.

### 5.2 Consequences of flawed block design on subsequent papers

The above strongly suggests that the output of the LSTM-based encoder trained by Spampinato et al. [31] does not constitute a “*brain-based visual object manifold*” [31, § 5 p. 6816]. Further, the analyses in § 3.8 and 3.9 strongly suggest that the object classifiers constructed by Spampinato et al. [31, § 3.3, § 4.2, and § 4.3] are not making use of *any* information in the output of the trained LSTM-based encoder, whether or not it contains a representation of human brain processing. Since these flaws are orthogonal to those of the data contamination issue, these methods are irreparably flawed and their shortcomings would not be remedied by correction of the contamination issue.

Kumar et al. [17] report a different EEG dataset that also appears to have been collected with a block design. Data was recorded from a single 10 s block for a single stimulus from each of 30 classes for each of 23 subjects. Each 10 s block was divided into either 40 or 200 segments. Ten-way cross validation was performed during analysis. We have no way of knowing whether the test sets contained segments from the same blocks that had segments in the corresponding training sets. But since a single block was recorded for each stimulus for each subject, the only way to avoid such would have been to conduct cross-subject analyses. The first analysis in § 3.7 suggests that such cross-subject EEG analysis is difficult and far beyond the current state of the art.

Tirupattur et al. [35] report using the dataset from Kumar et al. [17] to drive a generative adversarial network (GAN) in a fashion similar to Palazzo et al. [20]. That work performs five-way cross validation during analysis. Again, we have no way of knowing whether the test sets contained segments from the same blocks that had segments in the corresponding training sets, and avoiding such would have required cross-subject analyses that our experiments suggest are far beyond the current state of the art.

### 5.3 Consequences of using flawed EEG encodings as input to image synthesis

Palazzo et al. [20], Kavasidis et al. [15], and Tirupattur et al. [35] all purport to use the EEG encodings to generate images using a GAN that depict human perception and thought. Since we lack access to the code for any of these papers, we are unable to perform the kind of random data analysis that we perform in § 3.8 and 3.9 to evaluate these methods. Instead, here we analyze the result in Tirupattur et al. [35], using only the published synthesized images. We select this paper because it has the most extensive set of generated examples. Tirupattur et al. [35, abstract p. 950] state:

*While extracting spatio-temporal cues from brain signals for classifying state of human mind is an explored path, decoding and visualizing brain states is new and futuristic. Following this latter direction, in this paper, we propose an approach that is able not only to read the mind, but also to decode and visualize human thoughts. More specifically, we analyze brain activity, recorded by an ElectroEncephaloGram (EEG), of a subject while thinking about a digit, character or an object and synthesize visually the thought item. To accomplish this, we leverage the recent progress of adversarial learning by devising a conditional Generative Adversarial Network (GAN), which takes, as input, encoded EEG signals and generates corresponding images.*

Tirupattur et al. [35, § 1 p. 950] further state:

*Our goal is to extract some cues from the brain activity, recorded using low-cost EEG devices<sup>1</sup>, and use them to visualize the thoughts of a person. More specifically, we attempt to visualize the thoughts of a person by generating an image of an object that the person is thinking about. EEG data of the person is captured while he is thinking of that object and is used for image generation. We use a publicly available EEG dataset [16] for our experiments and propose a generative adversarial model for image generation. We make the following contributions in this work: 1) we introduce the problem of interpreting and visualizing human thoughts, 2) we propose a novel conditional GAN architecture, which generates class-specific images according to specific brain activities; 3) finally, we also show that our proposed GAN architecture is well suited for small-sized datasets and can generate class-specific images even when trained on limited training data.*

*We demonstrate the feasibility and the effectiveness of the proposed method on three different object categories, i.e., digits, characters, and photo objects, and show that our proposed method is, indeed, capable of reading and visualizing human thoughts.*

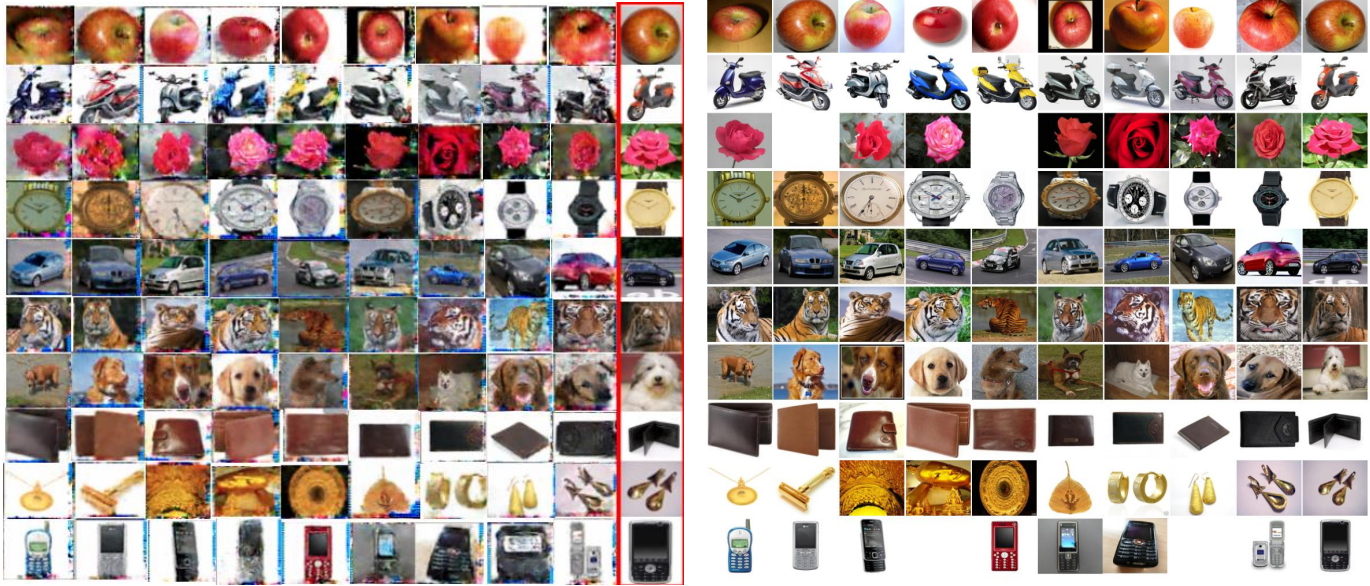


Fig. 4. (left) Fig. 6 from Tirupattur et al. [35] illustrating sample images purportedly generated by a GAN model from EEG encodings (except for the right column in red that illustrates a random image of the given class from the training data). (right) corresponding identical ImageNet images for almost all of the generated images. Note that some, but not all, of the purportedly synthesized images on the left are horizontal mirrors of ImageNet images on the right. Also note that all of the purportedly synthesized images contain the same precise fine-grained detail as the corresponding ImageNet images. In particular, each image not only depicts the corresponding class but also depicts the exact non-class-specific background as the ImageNet counterpart.

Conditional GANs are not intended to output exact copies of the training set because the input that leads to synthesized images contains noise in addition to class information. GANs in their true spirit are supposed to learn visual features that are indicative of different instances of objects within a class and synthesize novel images for instances of a class by selecting and combining those features in a semantically and visually coherent fashion. The current state-of-the-art [22] is unable to achieve this lofty goal. However, essentially all of the example images illustrated in Tirupattur et al. [35, Fig. 6] are nearly exact copies of images in ImageNet (Fig. 4). GANs typically do not generate such near exact copies. Moreover, in order for them to generate the same image twice, they must be provided with the same conditioning input, which in this case comprises both an EEG encoding and noise. It would be highly unlikely for the same EEG encoding and the same noise to be provided at each training iteration. Thus it would be highly unlikely for a proper conditional GAN to be able to memorize the training set. Moreover, it would be highly unlikely for the same EEG encoding and the same noise to be provided both during training and test. Thus it would be highly unlikely for a proper conditional GAN to output near exact copies of the training set during test. Without their code and data, it is impossible for us to precisely determine the cause of this highly unlikely circumstance. Nonetheless, this calls into question their claim that their *proposed method is, indeed, capable of reading and visualizing human thoughts*.

#### 5.4 Consequences for flawed joint training of EEG and image encoders to analyze brain processing of images

Palazzo et al. [21, Fig. 1] jointly train an EEG encoder and an image encoder to produce similar encoded representations and then purport to use the trained encoders for several

purposes: producing saliency maps [21, § 4, § 7.3, and Figs. 3 and 5], producing EEG activation maps [21, § 5, § 7.4, and Fig. 6], and associating EEG activity with layers in a synthetic object detector [21, § 6, § 7.4, and Fig. 9]. Since these results were all produced with the same contaminated dataset, these results are all suspect. Moreover, Tables 5 and 7 suggest that using the proposed methods to produce legitimate results from uncontaminated data collected with a rapid-event design is unlikely to succeed. Beyond this, however, the methods themselves appear to be fundamentally flawed and unlikely to demonstrate anything, even if they could be made to work on uncontaminated data. The loss function employed in the joint training regimen simply constrains the two encoded representations to be similar. A perfectly trained image encoder, trained against class labels, would simply encode image class, no more and no less. A perfectly trained EEG encoder, trained against class labels, would simply encode stimulus class, no more and no less. During joint training of the EEG encoder, the image encoder serves simply as a surrogate for class labels, no more and no less. Similarly during joint training of the image encoder, the EEG encoder serves simply as a surrogate for class labels, no more and no less. Thus joint training accomplishes nothing that could not be accomplished by training the components individually against class labels. The resulting encoded representations would contain no information beyond class labels. With this, the saliency map [21, Eqs. (3) and (4) and Fig. 5] measures nothing more than the degree to which image regions impact classification accuracy of an object detector trained against class labels. Brain activity, whether encoded in EEG data or not, plays no role in constructing these saliency maps. The importance  $I_c$  of an EEG channel  $c$  as rendered in activation maps [21, Eqs. (5–7) and Fig. 6] measures nothing more than the degree to which removing

the information in  $c$  decreases the classification accuracy, averaged over trials for a class and/or subjects. While this nominally is a valid approach, with the contaminated data collected with a block design, all these maps illustrate is the degree to which a given channel encodes the arbitrary long-term brain states associated with the block, not any class-specific information. Moreover, Tables 2–4, 6, and 8–10, suggest that any purported temporal information in Palazzo et al. [21, Figs. 7 and 9] is artifactual. Tables 5 and 7 suggest that activation maps computed with uncontaminated data collected with a rapid-event design would simply be blank, as accuracy would be at chance levels both prior and subsequent to removing the information in any particular EEG channel. Finally, association  $A_{c,l}$  between an EEG channel  $c$  and any component  $l$  of an object detector is simply a linear combination of the class-average activation maps [21, Fig. 6] weighted by the degree to which removing the portion  $l$  of an object detector causes misclassifications to a given class. This holds whether  $l$  is a portion of a feature map, an entire feature map, or all feature maps in a given layer, as computed by Palazzo et al. [21, Eqs. (8–10)] and rendered in Palazzo et al. [21, Fig. 9]. The fact that the activation maps in Palazzo et al. [21, Fig. 9] become more diffuse for later layers in an object detector says nothing more than the fact that removing later layers in an object detector leads to higher entropy in the output distribution, a property solely due to the image classifier and completely independent of any brain processing, whether measured by EEG or not.

## 5.5 Summary

In summary, our results call into question not only the results of Spampinato et al. [31] but other published results as well [8, 15, 17, 20, 21, 30, 35]. They do so in four distinct ways. First, they raise doubts about all claims that depend directly or indirectly on the ability to use the kinds of classification algorithms reported here, including the particular classification algorithm of Spampinato et al. [31], to extract class information from the particular data of Spampinato et al. [31]. That alone raises doubts about all of the above cited papers. Second, they raise doubts about the ability of the kinds of classification algorithms reported here, including the particular classification algorithm of Spampinato et al. [31], to extract class information from any EEG data collected with a block design. It places the burden of proof that there is no data contamination on any use of a block design. This raises doubts not just about the particular dataset collected by Spampinato et al. [31], but further about the experimental protocol proposed by Spampinato et al. [31]. Third, they demonstrate that a whole spectrum of classification algorithms do not work on a dataset collected with a rapid-event design that does not suffer from data contamination. This raises doubts about not just the dataset and protocol, but further about the analysis methods and algorithms. Fourth, § 3.8 and § 3.9 raise doubts about the general approach underlying the proposed methods and algorithms for using EEG data to advance computer vision. While we have employed the random-data attack to the particular methods of Spampinato et al. [31], we believe that they also can be applied to all of the methods in Palazzo et al. [20], Kavasidis et al. [15], Tirupattur et al. [35], and

Palazzo et al. [21] as well. We are hindered in our attempt to conduct this analysis by the fact that the authors have declined to release their code to us, despite requests, and the fact that the published papers lack sufficient detail to replicate their models.

## 6 CONCLUSION

The results in Tables 5 and 7 suggest that the ability to classify 40 object classes in image stimuli and 12 activity classes in video stimuli from an EEG signal is extremely difficult and well beyond the current state of the art. Moreover, the enterprise of using neuroimaging data to train better computer-vision systems, proposed by [1, § 8 p. 625] and [25, Fig. 2 and § 3 last ¶ p. 4068], requires more sophisticated methods than simply attaching a regressor to a pretrained object classifier and is also likely to be difficult and beyond the current state of the art. Both of these enterprises are the subject of substantial ongoing effort. When widely published [8, 15, 17, 20, 21, 30, 31, 35], inordinately optimistic claims can lead to misallocation of valuable resources and can sideline more modest but legitimate and important advances in the field. Thus, when the sensational claims are recognized as false, it is imperative that the refutation be widely publicized to appropriately caution the community.

## ACKNOWLEDGMENTS

This work was supported, in part, by the US National Science Foundation under Grants 1522954-IIS and 1734938-IIS, by the Intelligence Advanced Research Projects Activity (IARPA) via Department of Interior/Interior Business Center (DOI/IBC) contract number D17PC00341, and by Siemens Corporation, Corporate Technology. Any opinions, findings, views, and conclusions or recommendations expressed in this material are those of the authors and do not necessarily reflect the views, official policies, or endorsements, either expressed or implied, of the sponsors. The U.S. Government is authorized to reproduce and distribute reprints for Government purposes, notwithstanding any copyright notation herein.

## REFERENCES

- [1] A. Barbu, D. P. Barrett, W. Chen, N. Siddharth, C. Xiong, J. J. Corso, C. D. Fellbaum, C. Hanson, S. J. Hanson, S. Hélie, E. Malaia, B. A. Pearlmutter, J. M. Siskind, T. M. Talavage, and R. B. Wilbur. Seeing is worse than believing: Reading people’s minds better than computer-vision methods recognize actions. In *European Conference on Computer Vision*, volume 5, pages 612–627, 2014.
- [2] P. Bashivan, I. Rish, M. Yeasin, and N. Codella. Learning representations from EEG with deep recurrent-convolutional neural networks. *arXiv*, 1511.06448, 2015.
- [3] N. Bigdely-Shamlo, A. Vankov, R. R. Ramirez, and S. Makeig. Brain activity-based image classification from rapid serial visual presentation. *IEEE Transactions on Neural Systems and Rehabilitation Engineering*, 16(5): 432–441, 2008.

- [4] T. A. Carlson, H. Hogendoorn, R. Kanai, J. Mesik, and J. Turret. High temporal resolution decoding of object position and category. *Journal of Vision*, 11(10):9, 2011.
- [5] H. Cecotti and A. Graser. Convolutional neural networks for P300 detection with application to brain-computer interfaces. *IEEE Transactions on Pattern Analysis and Machine Intelligence*, 33(3):433–445, 2011.
- [6] C. Cortes and V. Vapnik. Support-vector networks. *Machine Learning*, 20(3):273–297, 1995.
- [7] J. Deng, W. Dong, R. Socher, L.-J. Li, K. Li, and L. Fei-Fei. Imagenet: A large-scale hierarchical image database. In *Computer Vision and Pattern Recognition*, pages 248–255, 2009.
- [8] C. Du, C. Du, X. Xie, C. Zhang, and H. Wang. Multi-view adversarially learned inference for cross-domain joint distribution matching. In *International Conference on Knowledge Discovery & Data Mining*, pages 1348–1357, 2018.
- [9] L. Fei-Fei, R. Fergus, and P. Perona. One-shot learning of object categories. *IEEE Transactions on Pattern Analysis and Machine Intelligence*, 28(4):594–611, 2006.
- [10] I. Goodfellow, J. Pouget-Abadie, M. Mirza, B. Xu, D. Warde-Farley, S. Ozair, A. Courville, and Y. Bengio. Generative adversarial nets. In *Advances in neural information processing systems*, pages 2672–2680, 2014.
- [11] Q. Gu, Z. Li, and J. Han. Generalized Fisher score for feature selection. *arXiv*, 1202.3725, 2012.
- [12] S. Hochreiter and J. Schmidhuber. Long short-term memory. *Neural Computation*, 9(8):1735–1780, 1997.
- [13] B. Kaneshiro, M. P. Guimaraes, H.-S. Kim, A. M. Norcia, and P. Suppes. A representational similarity analysis of the dynamics of object processing using single-trial EEG classification. *PloS One*, 10(8):e0135697, 2015.
- [14] I. Kavasidis and C. Spampinato, Sept. 5, 2018. Personal communication.
- [15] I. Kavasidis, S. Palazzo, C. Spampinato, D. Giordano, and M. Shah. Brain2Image: Converting brain signals into images. In *ACM Multimedia Conference*, pages 1809–1817, 2017.
- [16] D. P. Kingma and M. Welling. Auto-encoding variational bayes. *arXiv*, 1312.6114, 2013.
- [17] P. Kumar, R. Saini, P. P. Roy, P. K. Sahu, and D. P. Dogra. Envisioned speech recognition using EEG sensors. *Personal and Ubiquitous Computing*, 22(1):185–199, 2018.
- [18] M. Marszałek, I. Laptev, and C. Schmid. Actions in context. In *Computer Vision and Pattern Recognition*, pages 2929–2936, 2009.
- [19] S. Palazzo, Oct. 31, 2018. Personal communication.
- [20] S. Palazzo, C. Spampinato, I. Kavasidis, D. Giordano, and M. Shah. Generative adversarial networks conditioned by brain signals. In *International Conference on Computer Vision*, pages 3410–3418, 2017.
- [21] S. Palazzo, C. Spampinato, I. Kavasidis, D. Giordano, and M. Shah. Decoding brain representations by multimodal learning of neural activity and visual features. *arXiv*, 1810.10974, 2018.
- [22] T. Salimans, I. Goodfellow, W. Zaremba, V. Cheung, A. Radford, and X. Chen. Improved techniques for training gans. In *Advances in neural information processing systems*, pages 2234–2242, 2016.
- [23] I. Simanova, M. Van Gerven, R. Oostenveld, and P. Haagoort. Identifying object categories from event-related EEG: toward decoding of conceptual representations. *PloS One*, 5(12):e14465, 2010.
- [24] K. Simonyan and A. Zisserman. Very deep convolutional networks for large-scale image recognition. *arXiv*, 409.1556, 2014.
- [25] J. M. Siskind. Conducting neuroscience to guide the development of AI. In *Conference on Artificial Intelligence*, pages 4067–4072, 2015.
- [26] C. Spampinato, Sept. 10, 2018. Personal communication.
- [27] C. Spampinato, Nov. 7, 2018. Personal communication.
- [28] C. Spampinato, Nov. 13, 2018. Personal communication.
- [29] C. Spampinato, Nov. 14, 2018. Personal communication.
- [30] C. Spampinato, S. Palazzo, I. Kavasidis, D. Giordano, M. Shah, and N. Souly. Deep learning human mind for automated visual classification. *arXiv*, 1609.00344, 2016.
- [31] C. Spampinato, S. Palazzo, I. Kavasidis, D. Giordano, N. Souly, and M. Shah. Deep learning human mind for automated visual classification. In *Computer Vision and Pattern Recognition*, pages 6809–6817, 2017.
- [32] C. Spampinato, S. Palazzo, I. Kavasidis, D. Giordano, N. Souly, and M. Shah, Sept. 10, 2018. Personal communication.
- [33] A. X. Stewart, A. Nuthmann, and G. Sanguinetti. Single-trial classification of EEG in a visual object task using ICA and machine learning. *Journal of Neuroscience Methods*, 228:1–14, 2014.
- [34] S. Stober, A. Sternin, A. M. Owen, and J. A. Grahn. Deep feature learning for EEG recordings. *arXiv*, 1511.04306, 2015.
- [35] P. Tirupattur, Y. S. Rawat, C. Spampinato, and M. Shah. ThoughtViz: Visualizing human thoughts using generative adversarial network. In *ACM Multimedia Conference*, pages 950–958, 2018.
- [36] C. Wang, S. Xiong, X. Hu, L. Yao, and J. Zhang. Combining features from ERP components in single-trial EEG for discriminating four-category visual objects. *Journal of Neural Engineering*, 9(5):056013, 2012.



**Ren Li** received his B.S. (2016) in electrical engineering from University of Science and Technology of China in Anhui, China. He is currently pursuing his Ph.D. in computer engineering at Purdue University, IN, USA. His research interests include computer vision and machine learning, especially benefiting computer-vision systems from brain-derived information.



**Jared S. Johansen** received a B.S. in electrical engineering from Brigham Young University (2010) and an M.S. in electrical engineering and an MBA from the University of Utah (2012). He is currently a Ph.D. student in the School of Electrical and Computer Engineering at Purdue University. His research lies at the intersection of machine learning, computer vision, natural language processing, and robotics.



**Hamad Ahmed** received his B.S. in electrical engineering from University of Engineering and Technology Lahore, Pakistan. He is currently a Ph.D. student in the School of Electrical and Computer Engineering at Purdue University, IN, USA. His research interests lie at the intersection of machine learning and computer vision.



**Thomas V. Ilyevsky** received his B.S. in electrical and computer engineering from Cornell University in 2016. He is currently pursuing a Ph.D. in electrical and computer engineering at Purdue University. His research focuses on artificial intelligence, computer vision, and natural language processing in the context of human-computer interaction.



**Ronnie B Wilbur** has a BA (Rochester) and Ph.D. (UIUC) in Linguistics. She is Professor of Speech, Language, and Hearing Sciences in the College of Health and Human Sciences, and Professor of Linguistics in the College of Liberal Arts, at Purdue University. Prior to starting at Purdue in 1980, she was visiting faculty at University of Southern California and faculty at Boston University. She has been widely invited as Visiting Professor (Amsterdam, Graz, Zagreb, Paris ENS, Salzburg, Stuttgart) and has been

funded by both the National Science Foundation and the National Institutes of Health.



**Hari M Bharadwaj** is an Assistant Professor at Purdue University in the Department of Speech, Language, and Hearing Sciences, and the Weldon School of Biomedical Engineering. Hari received a B.Tech. in Electrical Engineering from Indian Institute of Technology, Madras, in 2006, and M.S. degrees in Electrical Engineering and Biomedical Engineering from the University of Michigan, Ann Arbor, in 2008. In 2014, he completed a Ph.D. in Biomedical Engineering at Boston University. Following post-doctoral work

at the Martinos Center for Biomedical Imaging at Massachusetts General Hospital, Hari joined the faculty at Purdue University in 2016, where his lab integrates a multidisciplinary array of tools to investigate the neural mechanisms underlying auditory perception in humans.



**Jeffrey Mark Siskind** received the B.A. degree in computer science from the Technion, Israel Institute of Technology in 1979, the S.M. degree in computer science from MIT in 1989, and the Ph.D. degree in computer science from MIT in 1992. He did a postdoctoral fellowship at the University of Pennsylvania Institute for Research in Cognitive Science from 1992 to 1993. He was an assistant professor at the University of Toronto Department of Computer Science from 1993 to 1995, a senior lecturer at the Technion

Department of Electrical Engineering in 1996, a visiting assistant professor at the University of Vermont Department of Computer Science and Electrical Engineering from 1996 to 1997, and a research scientist at NEC Research Institute, Inc. from 1997 to 2001. He joined the Purdue University School of Electrical and Computer Engineering in 2002 where he is currently an associate professor.